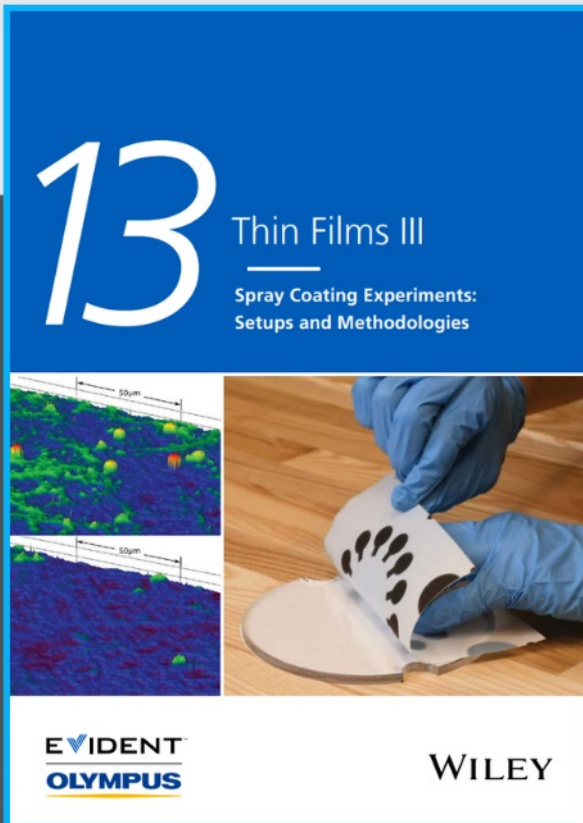# Spray Coating Experiments: Setups and Methodologies

The latest eBook from Advanced Optical Metrology. Download for free.

Spray Coating Experiments: Setups and Methodologies, is the third in our Thin Films eBook series. This publication provides an introduction to spray coating, three article digests from Wiley Online Library and the latest news about Evident's Image of the Year Award 2022.

Wiley in collaboration with Evident, are committed to bridging the gap between fundamental research and industrial applications in the field of optical metrology. We strive to do this by collecting and organizing existing information, making it more accessible and useful for researchers and practitioners alike.

13

Thin Films III

Spray Coating Experiments: Setups and Methodologies

EVIDENT OLYMPUS

WILEY

EVIDENT OLYMPUS

WILEY

Design of Stimuli-Responsive Peptides and Proteins

Yang Li, Guangze Yang,* Lukas Gerstweiler, San H. Thang, and Chun-Xia Zhao*

Stimuli-responsive peptides and proteins are an exciting class of smart biomaterials for various applications and have received significant attention over the past decades. A wide variety of stimuli such as temperature, pH, ions, enzymes, magnetic field, redox, etc., are explored. This article provides a review of five intensively studied types of stimuli-responsive peptides and proteins, their design principles and applications, including temperature-, pH-, light-, metal ion-, and enzyme-responsive with an emphasis on the key design concepts and switch function. Moreover, typical examples of their applications are discussed to provide a better understanding of the design concept and underlying methodology. This review will facilitate and inspire future innovation toward new peptide- and protein-based materials and their diverse applications.

1. Introduction

Developing novel biomaterials is a vibrant area of research with tremendous potential in various applications. Peptide- and protein-based materials are attractive due to their well-defined compositions, biodegradability, and the possibility of tuning their functionality by altering the amino acid sequence.[1] Stimuli-responsive biomolecules as an advanced class of materials have been extensively studied, because controlled conformational

Y. Li, G. Yang, L. Gerstweiler, C.-X. Zhao
School of Chemical Engineering and Advanced Materials
Faculty of Sciences
Engineering and Technology
The University of Adelaide
Adelaide 5005, Australia
E-mail: guangze.yang@adelaide.edu.au; chunxia.zhao@adelaide.edu.au
Y. Li, G. Yang, S. H. Thang, C.-X. Zhao
Australian Research Council
Centre of Excellence for Enabling Eco-Efficient Beneficiation of Minerals
Adelaide 5005, Australia
Y. Li, G. Yang, C.-X. Zhao
Australian Institute for Bioengineering and Nanotechnology
The University of Queensland
Brisbane 4072, Australia
S. H. Thang
School of Chemistry
Monash University
Melbourne 3800, Australia

changes can be induced or triggered by different stimuli. By virtue of the great diversity in the structural and physicochemical properties of amino acids, biomolecules with desirable stimuli responses and unique self-assembly functions can be constructed.[2] In addition, non-natural amino acids can be incorporated to further extend the scope.[3]

Various physical and chemical stimuli, such as temperature, pH, light, ions, enzymes, magnetic field, shear force, and redox reaction can be used to trigger the conformational changes of peptides or proteins. Among them, temperature, pH, and enzymes are the most intensively investigated response modes, while light as an alternative stimulus has attracted substantial attention as it can be spatially and temporally controlled without changing the microenvironment.[4]

Self-assembled biomolecules have been widely studied due to their unique features in various applications. Peptides and proteins can assemble into a range of nanostructures such as nanotubes, nanowires, nanofibrils, and nanovesicles that show superior functionality in terms of chemical diversity, biocompatibility, loading capacity, and specific binding ability.[5] The use of external stimuli to regulate the self-assembly of biomolecules contributes greatly to the control of their morphology and functionality.

Recent review papers mainly focus on certain specific applications such as drug delivery, cancer treatment, and peptide self-assembly, making its challenging for researchers who do not have expertise in biomolecule design and biomolecular engineering to embrace the tremendous potential of purposely designed stimuli-responsive biomolecules. This article aims to share the exciting recent advancements in the field, and provide a comprehensive overview of the underlying design concepts and principles, which will facilitate future design of more advanced biomolecule-based materials for various applications. Stimuli-responsive peptides and proteins are categorized into five groups responding to different external stimuli including temperature, pH, light, metal ions, and enzymes. For each platform, we discuss their design principles, explain their switch function, and highlight key aspects that facilitate their intended functions. In addition, we discuss typical examples of their applications in each category to further enhance a better understanding of the design concept and underlying methodology.

2. Temperature-Responsive Biomolecules

Temperature has been extensively explored as a stimulant to trigger the conformational changes of peptides and proteins.

**ADVANCED
SCIENCE NEWS**

www.advancedsciencenews.com

**ADVANCED
FUNCTIONAL
MATERIALS**

www.afm-journal.de

Increasing temperature initiates changes in their secondary and/or tertiary structures, thus leading to the disruption of their functions. For example, heat-induced denaturation is a useful tool to derive details on the thermodynamic stability of proteins.[3] This section describes the design principles and applications of temperature-responsive peptides and proteins.

2.1. Design Principles

2.1.1. Peptides

The stimuli-responsive properties of biomolecules rely on the design of amino acid sequence, the selection of certain motifs, and secondary or tertiary structures. α helices have been widely explored and used for peptide and protein design. A common strategy for designing thermoresponsive peptides and proteins is based on the α-helix to β-sheet transition. This transition is often driven by the hydrophilic–hydrophobic interactions involved in the helical structure.[3] For example, the heptad repeat, a very common motif, consists of a repeating pattern of 7 amino acids, *a b c d e f g*, which form two helical turns (**Figure 1**a). Each α-helix turn consists of 3.7 amino acids with a vertical unit of translation of 1.47 Å per residue.[6] Amino acids located at *a* and *d* positions of the heptad are hydrophobic including valine (Val), isoleucine (Ile), or leucine (Leu), creating a hydrophobic face on the α helix, while *b*, *c*, and *f* positions are normally hydrophilic or helix-inducing amino acids, making this face of the α helix hydrophilic. Replacing the hydrophilic amino acid at the *f* position with a hydrophobic one in a coiled-coil structure is able to accelerate the conformational change due to the formation of a hydrophobic patch in positions *d*, *f*, and *a*, thus resulting in the secondary structure transition from α-helix to β-sheet. The transition temperature (T_t) is dependent on the amino acid at the *f* position. For instance, substituting a serine (Ser) for a tyrosine (Tyr) (Figure 1b–d) decreases the transition temperature from 76 to 55 °C.[3,7] This kind of conformational transition from α-helix to β-sheet is often associated with various neurodegenerative diseases, therefore, has attracted huge research interest.

As opposed to the temperature-sensitive transition from α-helix to β-sheet, the peptide DARV16-IV (**Table 1**) is capable of undergoing a β-sheet to α-helix transition upon heating.[8] The peptide is composed of alternating hydrophobic and hydrophilic amino acid residues in the peptide chain. By varying pH or temperature, a conformational change occurs. It displays a β-sheet secondary structure at room temperature that transforms into α-helix without a random coil transition state upon heating up to 75 °C. Then it remains in a β-sheet conformation for weeks at room temperature before transforming back into the α-helix structure. Moreover, the change in the secondary structure leads to a 50% reduction in the peptide length from 5 to 2.5 nm. With such unique dual-responsive properties, DARV16-IV can be potentially adopted in biomedical applications such as peptide-based sensors and diagnostic devices that respond to in vitro or in vivo environmental changes.[8]

Another possible structural change is the shift in the handedness or "chiroptical switch" of the α-helix.[57] Nonapeptides adopt right-handed helical structures at ambient temperature by adding Boc-D-amino acids, but shift quickly into a left-handed helix upon cooling to 5 °C. They return their right-handed helical structure upon heating again. Trichogin (Tricol), a naturally occurring peptide with antitumor and antimicrobial activity, exhibits a reversible and thermoresponsive transition from a right- to a left-handed helix upon cooling when it is modified with a methyl ester or free carboxylic acid at its C-terminal.[9] The trichogin analogs such as L4-ol, and T8-OMe (Table 1) have been investigated over a broader temperature range from +20 to –87 °C. The temperature-driven conformational changes of all trichogin analogs are fully reversible. Undergoing the conformational shift, the antibacterial activity of trichogen analogues was significantly reduced.[9]

2.1.2. Proteins

Elastin-like polypeptides (ELPs), inspired by human tropoelastin, are one of the most extensively studied temperature-sensitive biomolecules.[58] ELPs are composed of oligomeric repeats of pentamer VPGXG, whereas X can be any amino acid except
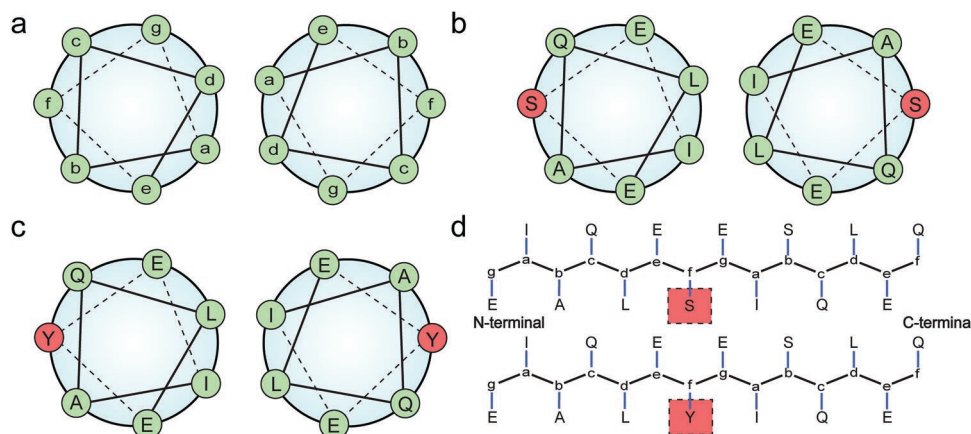

Figure 1. Structural illustration of heptad peptide design of a coiled-coil peptide. Coiled-coil representation a) consisting of two α helices. b) Ser at *f* position. c) Tyr at *f* position. Amyloid-like β-sheet arrangement patterns of d) linear sequences consisting of Ser and Tyr at the *f* position. Reproduced with permission.[3] Copyright 2010, American Chemical Society. Reproduced with permission.[7] Copyright 2007, American Chemical Society.

Table 1. Summary of temperature-, pH-, light-, metal ion-, and enzyme-responsive peptides and proteins.

Stimulus	Biomolecule name	Sequence	Transition point	Conformational changes	Refs.
Temperature	DARV16-IV	Ac-NH-ADADADADARARARAR-CONH$_2$	75 °C	β-sheet to α-helix	[8,9]
	L4-ol	nOct-Aib-GLLGGL-Aib-GI-Lol	−80 ± 20 °C	Reversible interconversion from right-to left-handed helix	[9]
	T8-OMe	nOct-Aib-GL-Aib-GGL-Toac-GIL-OMe	−49 ± 3 °C	Reversible interconversion from right-to left-handed helix	[9]
	ELP-HYD	MASMTGGQQMG-HHHHH-DDDDK-TVYAVTGRGDSPASSAA-[(VPGIG)$_2$-VPGKG(VPGIG)$_2$]$_3$VP	Room temperature	Formation of cross-linked hybrid ELP-hyaluronic acid (HA) when mixed with aldehyde-modified-HA	[10]
	CPP-ELP$_{BC}$	CPP 1 (Arg$_8$): RRRRRRRR; CPP 2 (TAT):YGRKKRRQRRR; CPP 3 (RTAT):YGRGGRRGRRR; ELP$_{BC}$:(VGVPG)$_{40}$-(AGVPGGGVPG)$_{30}$	37–42 °C	Unimers self-assemble to form micelles	[11]
	GLP1-ELP	AAHGEGTFTSDVSSYLEEQAAKEFI-AWLVKGAG-[(VPGAG)$_{60}$(VPGVG)$_{60}$]	30.2 °C	Soluble to ELP-rich coacervate	[12]
	Mixture of POP(V)-25% and ELP (V$_4$A$_1$)	POP(V)-25%:((GVGVP)$_{15}$-GD(A)$_{25}$K)$_4$ ELP(V$_4$A$_1$):(G[V$_4$/A$_1$]GVP)$_{80}$	Heating from 4 to 35 °C	Fruits-on-a-vine	[13]
	Mixture of POP (V$_1$A$_4$)-25% and ELP (V)	POP(V$_1$A$_4$)-25%:((G[V$_1$/A$_4$]GVP)$_{15}$-GD(A)$_{25}$K)$_4$ ELP(V):(GVGVP)$_{80}$	Heating from 4 to 35 °C	Core–shell	[13]
	M-B-ELP	M:C14; B$_1$: GAGASRGGSGGS; B$_2$: GAGAGAyRGGSGGSGGS; B$_3$: GLSL-SRGGSGGS; ELP: (GVGVP)$_{40}$ GY	20–25 °C	Reversible self-assembly into macroscopic objects	[14]
pH	pHcc	Ac-CGGGE-VSALENE-VAKLKNE-VKYLEAE-VARLKNE-VEFLEK-CONH$_2$	pH 4.1/10.5	Formation of coiled-coil structure	[15]
	IAAL E3/K3	E3: Ac-E(IAALEKE)$_2$IAALEK-NH$_2$ K3: Ac-K(IAALKEK)$_2$IAALKE-NH$_2$	pH 5/7	Partially unfolding of coiled-coil (pH 4) to stable coiled-coil (pH 7)	[3,16]
	AM1	Ac-MKQLADS-LHQLARQ-VSRLEHA-CONH$_2$	pH 3.6/7.4	Reversible shifting between forming stable foam and collapsing	[17]
	SurSi	Ac-MKQLAHS-VSRLEHA-RKKRKKRKKRKKGGGY-CONH$_2$	Increasing pH from 7 to 11.8	Interfacial tension is reduced as pH increasing	[18]
	DAMP4	MD(PSMKQLADS-LHQLARQ-VSRLEHA)$_4$	pH 7.5/8.5	Reversible shifting between forming stable foam and collapsing	[19]
	P11-2	CH$_3$CO-QQRFQWQFEQQ-NH$_2$	pH 5	Form stable nematic gels (pH < 5), destabilizing at higher pH	[20]
	EAK-12d	AEAEAEAEAKAK	pH 3–5	α-helix to β-sheet	[21]
	SgI	GSFSIQYTYHV	pH 6–10	Gel formation	[22]
	KD	AcNH-KGSFSIQYTYHVD-CONH2	pH 7	Random coil to β-sheet rich nanofibril	[23]
	A1H1	AATAVSHTTHHA	Shift from neutral to acidic pH	Stability of A1H1 β-sheet is reduced and disassembling to random monomers at lower temperatures	[24]
	KPK	Poly($_L$-K)-b-poly (propylene oxide)-b-poly ($_L$-K)	pH 3–7	Random coil to spherical micelle in acidic condition, helix to vesicle or disk micelle in basic condition	[25]
	PLGA–PEG–H$_7$K(R$_2$)$_2$	PLGA–PEG–RRK(HHHHHHH)RR	pH 7.4	Self-assemble into polymeric micelles containing PTX (PEX-PM) at neutral pH, expose K(R$_2$)$_2$ to the surface when pH reduces below 7.4 (acidic)	[26]
	PA1	C$_{16}$H$_6$-OEG	pH 6–6.5/7.5	Self-assemble into nanofibers at pH 7.5 and disassemble at pH 6–6.5	[27]
	PA2	OEG-H$_6$K(C$_{12}$)	pH 6–6.5/7.5	Self-assemble into nanospheres at pH 7.5 and disassemble at pH 6-6.5	[27]
	MAX1	VKVKVKVKV^{D}PPTKVKVKVKV-NH$_2$	pH 9	Self-assemble into a β-hairpin structure	[28]
	Fc-FF	Fc-FF	pH 5.9	Self-assemble into nanohelices	[29]

**ADVANCED
SCIENCE NEWS**

www.advancedsciencenews.com

**ADVANCED
FUNCTIONAL
MATERIALS**

www.afm-journal.de

Table 1. Continued.

Stimulus	Biomolecule name	Sequence	Transition point	Conformational changes	Refs.
	C_{12}-GGSK	Lauroyl-G-G-$_D$-S-$_D$-C(TFA)-NH$_2$	pH 3/8	Self-organized into micelles (pH 3), and fibers (pH 8)	[30]
	KLD-12	AcN-KLDLKLD-LKLDL-CNH$_2$	pH 7.4	Random coil to β-sheet	[31]
Light	SUP-Azo	GAGP[(GVGVP) (GKGVP)$_9$]$_2$GWPH$_6$-Azo	UV	Reversible Z- to E- isomerization	[32]
	uAA	VPGGGVPG-Azo-uAA (1/2/3)-GVPGGGK	Azo-uAA 1: blue or UV light, Azo-uAA 2 and 3: blue or green light	Self-assembly into nanostructures	[33]
	CPA	pNBMA$_{25}$-CP-pPEGA$_{27}$	UV	Disassembly	
	P20	PDMNBLG$_{44}$-r-PVBLG-8$_{175}$	UV/NIR	Disruption of α-helical structure	[34]
Ions	DLeu	GSARDDLLLGDAGANLLLGLAGNDLLLG-GAGDDLLLGDEGSDLLLGDAGNDLLLG-GQGDDLYLFGVGYGHDLILESGGGHDTIR	Calcium (0.9–1.2 mm)	Disordered to β-roll	[35]
	406	GSARDDVLIGDAGANSLVGLAGNDV-LSGGAGDDLLLGDEGSDLLSGDAGNDVLD GGQGDDTYLFGVGYGHDRIVESGGGH-DTIRINAGADQLWFARQGNDLEIRILGTD DALTVHDWYRDADHRVEIIHAANQAVDQ-AGIEKLVEAMAQYPD	Calcium (0.9–1.2 mm)	Disordered to β-roll	[35a]
	P(EG$_x$DMA-Glu)	P(EG$_x$DMA-Glu)$_{50}$ (x = 1–3)	Sodium chloride (maximum helicity at 120 mm)	Random coil to α-helix	[36]
	JR2EC	NH$_2$-NAADLEKAIEALEKHLEAKG-PCDAAQLEKQLEQAFEAFERAG-COOH	Zinc (0.5 mm)	Helix-loop-helix to four-helix bundles	[37]
	IH6	Ac-ILVAGH-NH$_2$	Ag$^+$ (1:2 silver to IH6)	Antiparallel to parallel β-sheet assembly	[38]
	L9	Ac-(3′-PyA) LRLRLRL (3′-PyA)-CONH$_2$	Ag$^+$ (1.88 mm)	Self-assemble into β-sheet	[39]
	BP	B(OH)$_2$FFFRGD-OH	Cu^{2+} (dose-dependent, experiments were conducted at 0–16 µm)	ARS/BP complex changes from nanpsheres to nanpfibers	[40]
Enzyme	BPC	[berberrubine]-PLG/VRKLVFF-[chlorin e6]	MMP-2	Cleavage followed by transition from nanoparticles to nanofibers	[41]
	Nap-FFGPLGLARKRK	[β-Naphthylacetic acid]-FFGPLG/LARKRK	MMP-7	Cleavage	[42]
	MePEG-peptide-PET-PCL	[PEG]-GPLG/IAGQRRRRRRRR-[pentaerythritol-ε-caprolactone]	MMP	Cleavage	[43]
	GLD; GLE; LGD; LGE	[EG]$_8$-Peptide-[EG]$_5$-C-[Au NPs] GPKG/LRGD (GLD), GPKG/LRGE (GLE), GPKLGRGD (LGD), and GPKLGRGE (LGE)	MMP-9	Cleavage followed by nanoparticle assembly	[44]
	AuNR@Res	[Au nanorod]-CCVVGRK-KRRQRRRPQGGPLG/VEKEKEKEK	MMP-9	Cleavage	[45]
	Dendrimer-GEM	[mPEG]-GFLG-[gemcitabine]	Cathepsin B	Cleavage	[46]
	AYR	[Ac]-AAAAAA-phosphorylated Y-RGD-[NH$_2$]	Alkaline phosphatase	Cleavage followed by transition from nanoparticles to nanofibers	[47]
	PSGMR	[Tetraphenylethene pyridinium]-[Propargylglycine]-KLVFF-GGG-SAVLQ/SGFRKMA-GGG-RRRRRR	Main protease	Cleavage followed by nanoparticle assembly	[48]
	AmpFQ-ETGE	LQLDEETGEFLPIQ-FF-[Quinone propionic acid]-FF	NAD(P)H quinone dehydrogenase 1	Cleavage followed by transition from nanoparticles to nanofibers	[49]
	Au-RRVR	[Au nanoparticle]-RRVR	Furin	Cleavage followed by nanoparticle assembly	[50]
	FBA-VKVKVK	[4-Formylbenzamide]-V/KV/KV/K	Human neutrophil elastase	Cleavage	[51]
	SA–DEX–PVGLIG–CUR	[Sialic acid–dextran]–PVG/LIG–[Curcumin]	MMP-2	Cleavage	[52]
	PPA	GPLG/LAGGWERDGS-[Polynorbornene]	MMP-2/MMP-9	Cleavage followed by transition from nanoparticles to network-like assemblies	[53]

**ADVANCED
SCIENCE NEWS**

www.advancedsciencenews.com

**ADVANCED
FUNCTIONAL
MATERIALS**

www.afm-journal.de

Table 1. Continued.

Stimulus	Biomolecule name	Sequence	Transition point	Conformational changes	Refs.
	TSP	(GGYGPGQQGPGGYGPGQQGPSGPGS AAAAAAAA)$_2$-HHHHHHDDDDKGFDPR/ GFPAGG	Thrombin	Cleavage	[54]
		FEFK and FEFEFKFK	Thermolysin	Gelation	[55]
		Ac-KYLAYPDSVHIWGGGSSKYQS-[TGX-D1]	Prostate specific antigen	Cleavage	[56]

proline (Pro).[59] At the temperature below the lower critical solution temperature (LCST), they exhibit a random coil structure and are soluble in aqueous solutions.[60] Upon heating, ELPs go through a conformational shift from a random coil to a β-spiral, followed by a "twisted filament" as the transition temperature (T_t) is reached (**Figure 2**). Once the temperature is above its T_t, ELPs aggregate and precipitate. Although the T_t of ELP biomolecules is a single temperature, the phase transition normally completes within a narrow temperature range of ≈2 °C.[60] By virtue of their unique temperature-responsive phase transition property, ELPs have been widely explored for various applications such as injectable controlled-release depots,[12a,61] tissue engineering scaffolds,[14,62] thermally triggered targeting of tumors,[58a] and purification tags for fusion proteins.[63]

The T_t depends primarily on the composition, molar fraction, and length of ELPs. It can be precisely tuned to the targeted temperature range at the molecular level by varying two orthogonal and genetically encoded variables of the ELPs, that is, the composition of X and the chain length.[64] Replacing the X in the pentamer with hydrophobic amino acid residues can reduce the transition temperature, while substituting X with polar or charged amino acids raises the T_t.[60] Moreover, the fusion of ELP to a target protein at the genetic level, also known as " ELPylation", has been widely adopted in designing new materials for various applications.[65] The molecular weight of the ELPs also plays a significant role. Longer ELPs exhibit lower transition temperatures compared to shorter ELPs with the same composition of X.[60] In addition, the LCST can be manipulated by varying external factors including concentration and ionic strength.[3] Kosmotropic anions polarize interfacial water molecules that hydrate amide groups on ELPs, thus decreasing the LCST. On the contrary, chaotropic anions lower the LCST due to the interfacial effect.[66]

2.2. Applications

Temperature responsive ELPs have been designed as a purification tag (**Figure 3**a) enabling the purification of target proteins through inverse transition cycling (ITC).[67] As the properties of ELPs can be retained even fused to various functional proteins, ELP fusion proteins can be separated by centrifuging cell lysates above T_t and then resolubilizing to form soluble purified ELP fusion proteins. The target protein can be harvested by cleavage at the fusion site through protease digestion or self-cleavage reaction (Figure 3b).[68] For example, proteins such as sfGFP, β-lactamase, streptokinase, and maltose-binding protein have been purified using self-cleaving ELP tags with yields of 200–340 µg mL^{-1}.[69] ITC can be used in postexpression purification of recombinant proteins, separation of reactants, and enzyme recycling that can be scaled up to meet industrial demands and offer simple, fast, and economic benefits.[70] Compared to polymers, recombinantly synthesized peptides have a defined length and hence a monodisperse population.[71] Also, ELPs can be conjugated with bifunctional groups such as drugs, signaling agents, ligands or binding moieties at the target site in the designed sequence without compromising their thermal responsive behavior.[60,72] Another important aspect is that ELPs are biodegradable that offers a more sustainable approach when compared to polymer-based materials.[73]
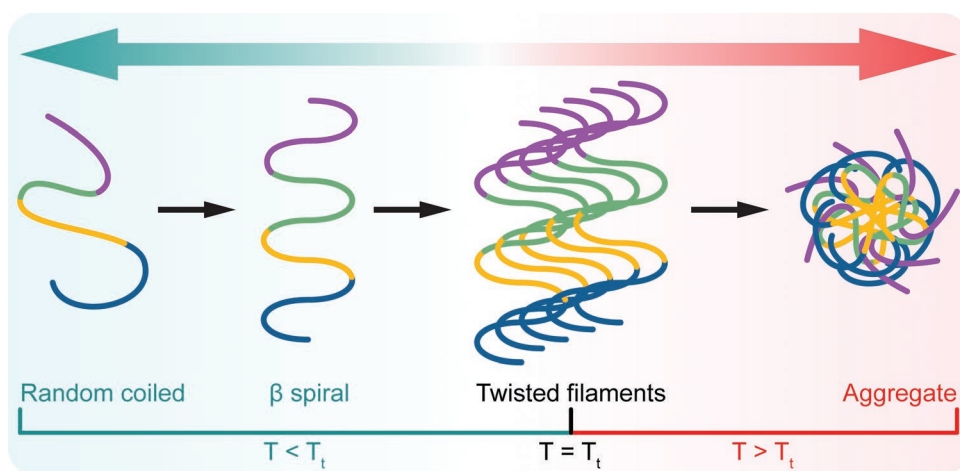

Figure 2. Conformational changes and aggregation upon temperature changes. Below the transition temperature (T_t), ELPs are in random coils. As temperature increases, they form a β-spiral structure followed by the formation of twisted filaments at T_t. ELPs aggregate and precipitate when reaching a temperature above T_t.
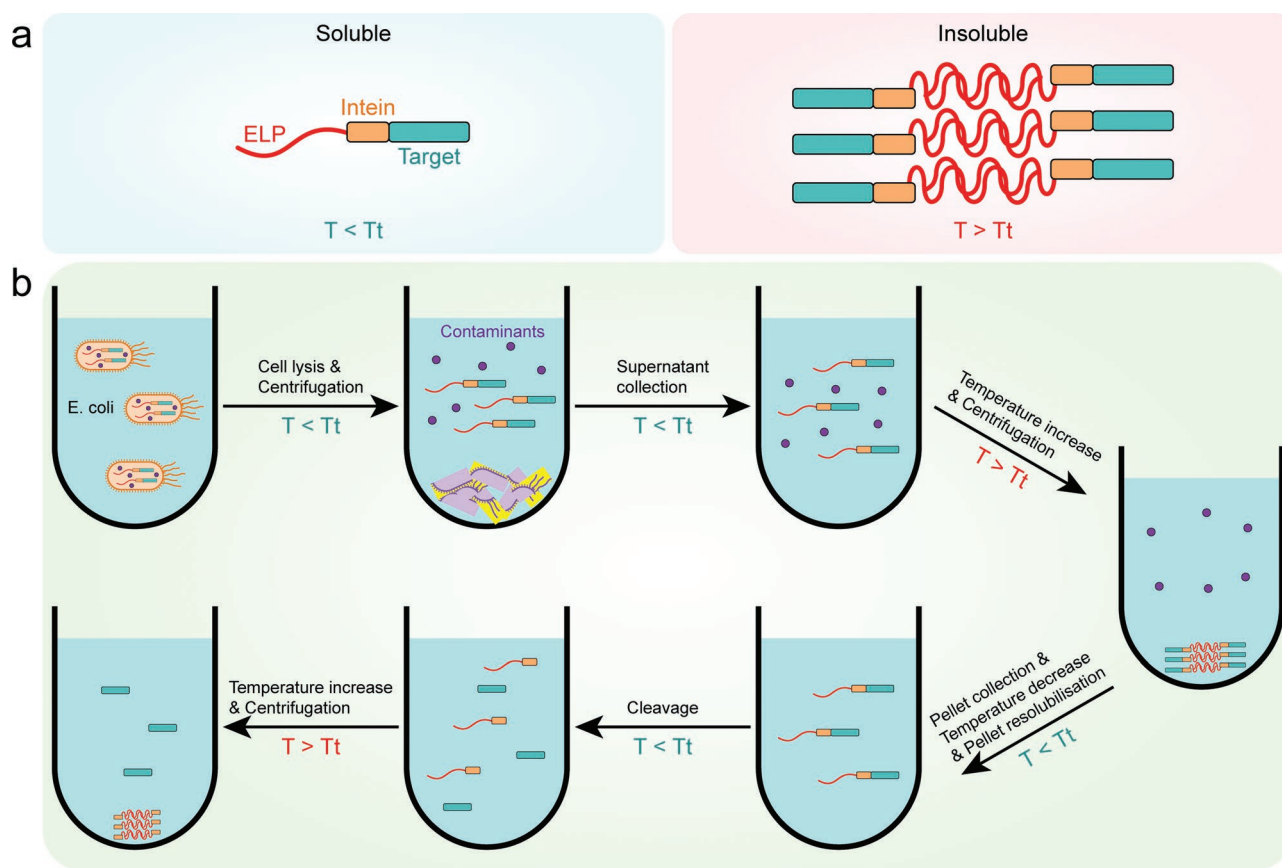
Figure 3. ELP as a purification tag. a) Temperature-responsive structure and solubility of ELP-intein tag fused to a target protein. b) The purification process of the target protein using ELP as the purification tag through inverse transition cycling (ITC).

ELPs have also been extensively studied for tissue engineering applications in cartilage regeneration, vascular graft, cell-sheet, ocular, and liver tissue engineering owing to their tuneable physiochemical properties and biocompatibility.[71,74] By incorporating peptide sequences for cell recognition and cross-linking, ELPs have been designed capable of modifying cell adhesion and tissue mechanical properties to imitate their native biological substrates. ELP block copolymers have also been developed with alternating hydrophobic and hydrophilic blocks and crosslinking domains that allow the modification of various features such as swelling, duration and viscoelastic properties.[74a] Moreover, ELPs can be cheaply produced via a shake flask culture or high-density fermentation making it viable for their practical applications.[62,74a,75]

ELP-hyaluronic acid (ELP-HA) hydrogels were designed for cartilage regeneration.[10] They were generated by dynamically adjusting the hydrazone bonds between aldehyde-modified HA and hydrazine-modified ELPs (ELP-HYD) (Table 1, **Figure 4**a). Chondrocytes were encapsulated in the ELP-HA hydrogels with different HA concentrations of 1.5%, 3% or 5%, showing that an increased HA concentration enhanced the gene expression of cartilage markers and sGAG deposition while avoided the formation of the fibrocartilage phenotype. Chen et al. investigated the ELP-modified silk fibroin (SF) for osteochondral repair.[76] A widely used physical crosslinking method, dehydro-thermal (DHT) treatment, was adopted to crosslink ELP with

SF fibers forming the S-ELP-DHT scaffold, which was found to promote the spreading and proliferation of bone mesenchymal stem cells (BMSCs) and chondrocytes. Both in vitro and in vivo experiments showed that S-ELP-DHT accelerated the formation of mature bone and cartilage tissue compared to SF-based materials (Figure 4b). The LCST phase behavior of ELPs can be further explored for filling a void or defect.[74a] Upon injection, the ELP solution forms an insoluble coacervate at a T_t below 37 °C and fills the defect.[74a] Betre et al. reported ELPs with a transition temperature of 35 °C.[77] The primary chondrocytes were entrapped in the ELP solution when reaching 35 °C, and the accumulated matrix can be recovered after 10 days through agitation at room temperature. More applications of ELPs in tissue engineering have been reviewed by Nettles et al.[78] and Varanko et al.[71]

ELPs are attractive in drug delivery as they can respond to external temperature changes that trigger their shift in structure, thus enabling targeted delivery or controlled uptake.[79] For example, the hyperthermic condition of inflamed pathological sites and tumor tissue can act as an internal stimulus to enable targeted drug delivery. Ideal targeted drug delivery should provide low affinity at health tissue while shift to a high avidity state at the diseased site via external trigger. Such approach was termed dynamic affinity modulation (DAM) that capable to switch between the high and low affinity states, known as "on" and "off" states, that allows a selective accumulation at the
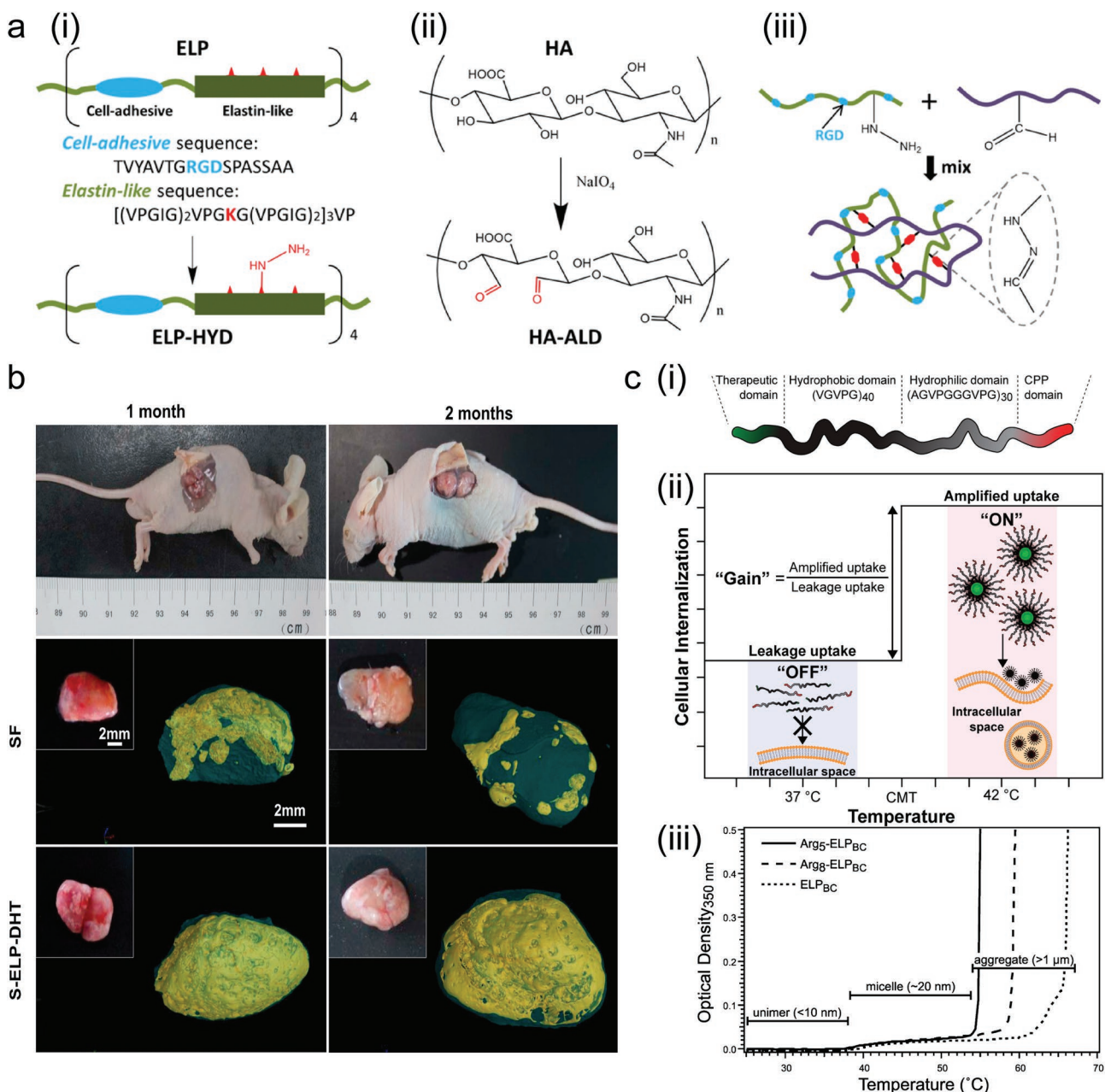
Figure 4. Applications of ELPs a) (i) ELP-modified sequence consists of a cell-adhesive (blue), temperature responsive ELP sequence (green), and lysine (Lys) residues (red) to generate ELP-HYD. (ii) Synthesis of aldehyde-modified hyaluronic acid (HA-ALD). (iii) Formation of ELP-HA hydrogel through the dynamic covalent linkages between ELP-HYD and HA-ALD. Reproduced with permission.[10] Copyright 2017, Elsevier. b) In vivo experiments in nude mice illustrate the bone regeneration by comparing BMSC-seeded SF and S-ELP-DHT scaffolds. The micro-CT images were used to analyze the new bone tissue (yellow). Reproduced with permission.[76] Copyright 2020, Elsevier. c) (i) Design of ELP$_{BC}$ nanopeptifier by connecting a CPP domain to ELP$_{BC}$ sequence. (ii) Switch between "off" and "on" states, at hyperthermic site (42 °C), unimers self-assemble to form micelles and display CPPs on the micelle corona. (iii) Characterization of CPP-ELPs via turbidimetry by using the solution concentration of 15 μM as an indication of size aggregation. Reproduced with permission.[11] Copyright 2014, American Chemical Society.

target sites.[80] Adopting the DAM phenomenon, MacEwan and Chilkoti designed nanopeptifier-based nanocarriers for controlled intracellular delivery of cancer drugs.[11] Cancer cell-penetrating peptides (CPPs) were incorporated, and their density can be modulated by using critical micellization temperature of ELPs (Table 1, Figure 4c). These ELP molecules self-assemble and promote the accumulation of ELP-based therapeutics at the

tumor sites due to the hyperthermic temperature (42 °C) while remaining as unimers at healthy sites with a body temperature of ≈37 °C.

Luginbuhl et al. reported a novel treatment strategy for type 2 diabetes by fusing the glycagon-like peptide-1 (GLP1) receptor to a thermosensitive ELP.[12] Native ligand for GLP1 receptor has a short half-life due to enzymatic inactivation

and rapid clearance. By contrast, the proposed novel treatment method offers a zero-order release kinetics with a circulation time up to 10 days or 17 days in mice or monkeys, respectively. These GLP1-ELP fusions (Table 1) were designed and expressed with a transition temperature span of 15 to 36 °C while remaining at or below the subcutaneous temperature of C57Bl/6J mice. The optimized GLP1-ELP fusions were able to promote therapeutic results by eliminating peak-and-valley pharmacokinetics and improve the overall safety and tolerability.

In addition to their biomedical applications, EPLs have also been explored for making novel biomaterials. Recent innovation has been made in building complex microparticle architectures by employing ELP-based intrinsically disordered proteins (IDPs).[13] IDPs are a class of nontoxic and biocompatible microparticles with biased amino acid composition and low sequence complexity.[81] ELPs as a typical class of IDPs have been extensively studied.[82] Roberts et al. reported a unique "fruits-on-a-vine" and a "core–shell network" architectures by establishing periodically spaced regions within an IDP that can modify the internal microarchitecture of the coacervate with control over the cloud point temperature (T_{cp}) of ELPs (Table 1).[13] These partially disordered polymers (POPs) demonstrated a lower T_{cp}-cooling than T_{cp}-heating due to the excess energy needed to overcome the hydrophobic interactions involved in the oligoalanine domains. Different ratios of Alanine (Ala) and Val were used at X position in the ELP sequence to modify the T_{cp} within the range of 20–50 °C. In addition, they could self-assemble into fractal-like microporous structure with adjustable stiffness and porosity. These rationally designed IDPs that can be readily integrated with conventional microfluidic polymer to develop novel biomaterials. Post-translational modification has been used to explore the diversity of ELP-based materials whereas the various transformations taken place within cells diversify the proteome.[83] The Chilkoti's group recently reported a temperature responsive fatty-acid-modified ELPs (FAME) hybrid materials, M-B-ELP (Table 1) using a one-pot recombinant expression and post-translational lipidation method.

3. pH-Responsive Biomolecules

pH-responsive peptides and proteins are triggered by pH change as a consequence of protonation or deprotonation.[3] pH stimuli often result in the switching in the secondary structures as well as the corresponding properties of biomolecules.

3.1. Design Principles

3.1.1. Peptides and Proteins

pH-sensitive peptides and proteins often exhibit α-helical structures. The manipulation of pH permits control of secondary structures leading to the formation of switchable assemblies such as coiled structures.[84] The incorporation of acidic and basic amino acids capable of being protonated or deprotonated by changing pH enables dynamic control over their conformational changes.[85] For example, a homodimeric coiled-coil α-helix peptide pHcc (Ac-CGGGE-VSALENE-VAKLKNE-VKY-LEAE-VARLKNE-VEFLEK-CONH$_2$) is composed of heptad repeats having Leu at the position d and glutamic acid (Glu) at the positions e and g (Table 1, **Figure 5**).[15] For pH < 4.1 (pK_a of Glu), the Glu residue is neutral, resulting in coiled-coil assembly driven by hydrophobic interaction, while for pH > 10.5 (pK_a of Lys), the Glu and Lys have opposite charges resulting in their electrostatic repulsion, thus disrupting the formation of coiled-coil structure. Therefore, the electrostatic interaction between Glu and Lys at positions e and g plays an important role in stabilizing the coiled-coil structure. Similarly, a pH-responsive heterodimeric coiled-coil system consists of two motifs IAAL E3/K3 (IAALEKE, IAALKEK) (Table 1).[3,16] The incorporation of oppositely charged Lys and Glu residues provides an electrostatic attraction for stabilizing the heterodimers at neutral pH and enables the manipulation of the heterodimeric stability via pH. At pH 5, the coiled-coil structure partially unfolds, while it associates into a stable coiled-coil structure at pH 7. The pH-responsive property stimulated by a small change in the physiologically relevant pH makes the
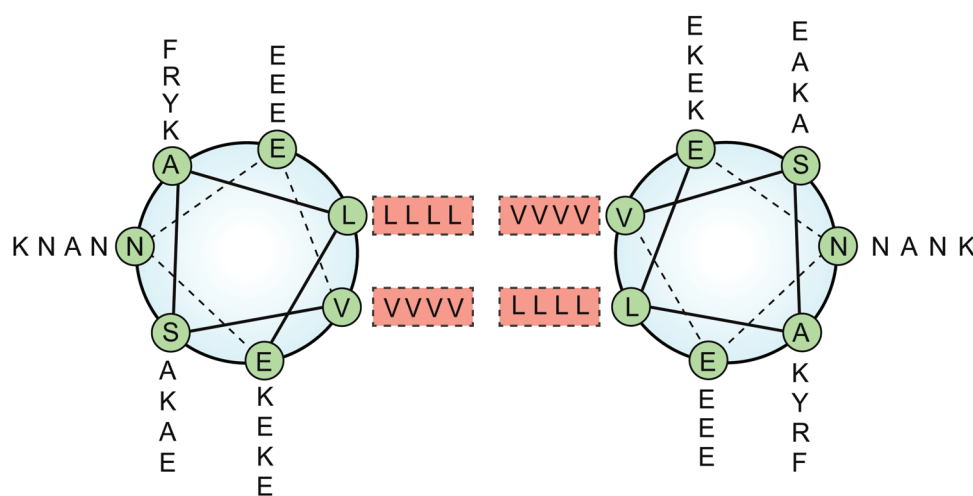

Figure 5. Representation of a pHcc peptide with a helical wheel structure consisting of two coiled-coil homodimers arranged in parallel. Reproduced with permission.[15] Copyright 2005, Royal Society of Chemistry.

E3/K3 attractive for controlled drug delivery applications such as intracellular drug release.

α-helical peptides can be designed to be amphiphilic with one phase being hydrophobic and the other hydrophilic when assembling at the air–liquid or liquid–liquid interface. The peptide AM1 (Ac-MKQLADS-LHQLARQ-VSRLEHA-CONH$_2$) with three heptads is a stimuli-responsive peptide surfactant (Table 1).[17] It was designed based on the amphipathic peptide Lac21 derived from bacteria in nature with the substitution of amino acids at positions 9 and 20 with two histidines (His) to enable the formation of metal ions mediated crosslinking.[17a] When it is dissolved in solutions, it has a random coil structure. By contrast, when it adsorbs at an oil–water interface, it assembles into an α-helical structure. The interfacial activity can be actively controlled and switched between a film state and a mobile detergent state by changing pH or adding metal ions.[17a] This special property allows the formation of foams or oil-in-water emulsions with stimuli-responsive properties that can be potentially applied in various fields.[86]

Several bifunctional peptides and proteins have been designed based on the AM1 peptide for its surface activity and stimuli-responsive features by modularizing the peptide AM1 with other functional sequences.[18,19,86b,c,87] AM-S is made of two modules including an AM1, the α-helical module, and a hydrophobic tail (GAGAGAGY) that helps to anchor it better at the air–water interface to improve foam stability.[86b,c] A bimodular catalytic peptide, SurSi (Table 1, **Figure 6**a), consists of a Sur module originating from AM1 to stabilize oil–water interfaces, and a Si module (RKKRKKRKKRKKGGGY) contributing to the catalytic synthesis of a silica shell thus forming an oil-core silica–shell nanocapsule.[18,88] In addition, to further reduce the production cost of AM1, a four-helix bundle protein DAMP4 (Table 1, Figure 6b) was designed that can be produced on a large scale in *Escherichia coli*.[19] It has a similar surface activity to AM1 as well as the pH-responsive property.

β-sheet peptides can also be designed with pH-sensitive properties. The β-sheet structures often lead to the formation of fibril-assembled hydrogels. The side chains of amino acids can be specifically modified to manipulate the electrostatic interactions among neighboring peptides. A peptide P11-2 consisting of 11 amino acids (CH$_3$CO-QQRFQWQFEQQ-NH$_2$) forms a β-sheet structure (Table 1).[20] Arginine (Arg) at position 3 and Glu at position 9 are incorporated to facilitate the formation of tape-like aggregates via electrostatic attractions between adjacent antiparallel β-strands. The phenylalanine (Phe), tryptophan (Trp), and Phe residues located at positions 4, 6, and 8, respectively, provide the hydrophobic adhesive stripe to enhance the association of tapes into ribbon structures. The P11-2 forms stable nematic gels at pH < 5 due to the net
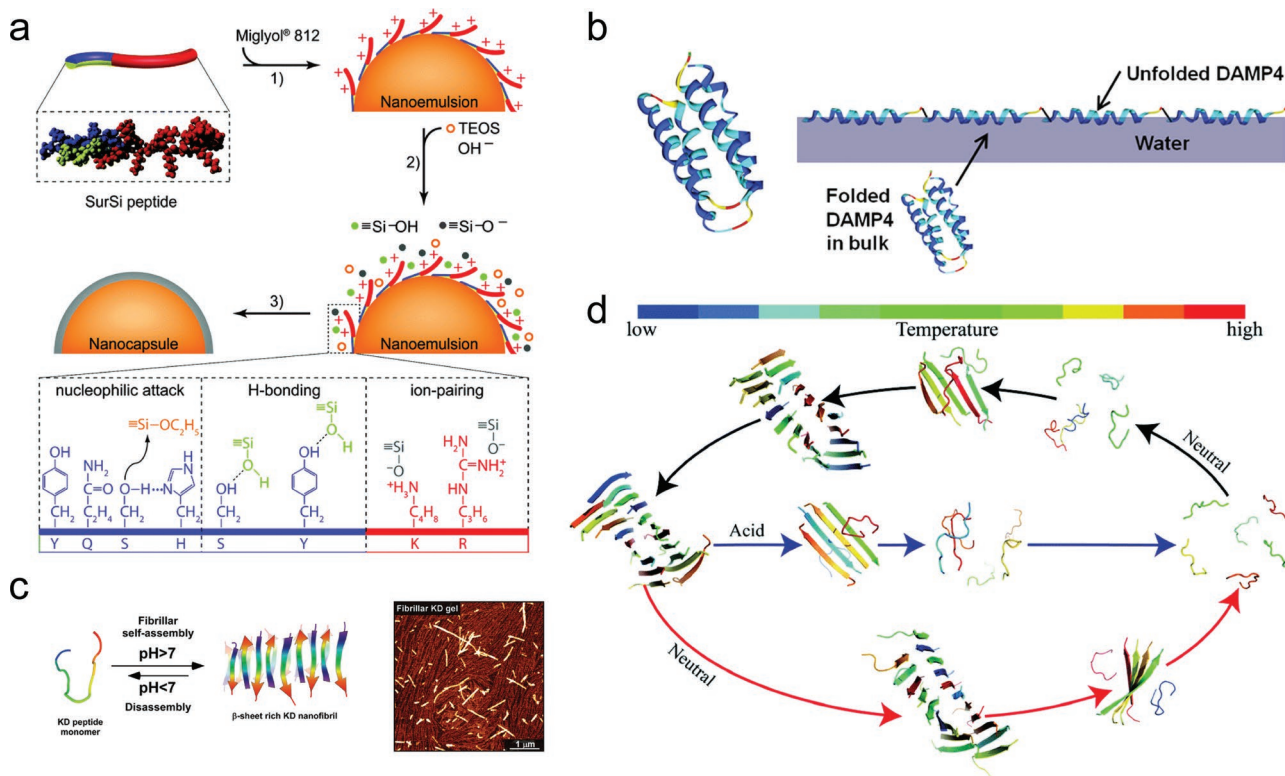

Figure 6. a) Synthesis of silica nanocapsules by using SurSi. Reproduced with permission.[89] Copyright 2014, Royal Society of Chemistry. b) Four-helix bundle DAMP4 consisting of 4 repeats of pH-responsive AM1 motifs. Reproduced with permission.[19] Copyright 2011, Wiley-VCH. Reproduced with permission.[90] Copyright 2014, Elsevier. c) Schematic diagram of the KD peptide reversibly assembling into fibrils in the presence of pH changes (left). AFM image of the KD gel with a scale bar of 1 μm (right). Reproduced with permission.[23] Copyright 2021, Wiley-VCH. d) Illustration of thermal hysteresis of A1H1 protein and its disassembling process facilitated by pH reduction. Reproduced with permission.[91] Copyright 2020, Royal Society of Chemistry.

positive charge from Arg,[20] while at higher pH, the fibrils flocculate and destabilize the gel.

Alternatively, tuning hydrophobic and hydrophilic interactions provides another powerful tool for controlling the conformational change of β-sheet. A number of self-assembled peptides have been designed to switch from β-sheet to α-helix in a pH-dependent manner based on hydrophobic and hydrophilic interactions.[21] EAK-12d (AEAEAEAEAKAK) (Table 1) has a cluster of negatively charged residues Glu toward the N-terminus, and it can transform from β-sheet to α-helix in response to pH. At pH 1–3, it forms the β-sheet conformation and experiences a structural transition to α-helix at pH 4. It undergoes a completely structural transition with ≈30% helical content when the pH is increased to 5.[21] The SgI peptide (GSFSIQYTYHV) (Table 1) derived from human semenogelin I (residues 38–48) has a sequence of alternating hydrophilic and hydrophobic residues.[22] The gel reveals a network of fibrils (4 nm diameter and length >1 µm). The peptide solution turns to hydrogel at pH 6–10, with the strongest gel forming at the isoelectric point of 7.8. Flanking two residues, Lys and aspartic acid (Asp), at the ends of SgI form the KD peptide sequence of KGSFSIQYTYHVD (Table 1, Figure 6c).[92] Dominated by secondary nucleation, the KD peptide can self-assemble into a fibrillar gel.[23] Moreover, it forms a pH-dependent gel composed of β-sheet fibrils with an optimal structure at pH 8 due to the lowest absolute net charge. And it slowly disassembles as the pH is reduced leading to the secondary structure change from ordered β-sheet to peptide monomers. Based on the KD peptide, microgel particles can be generated in a microfluidic device using the water-in-oil droplet template.

Suckerin protein family discovered in squid ring teeth inspires the design of a novel class of biomolecule-based materials with self-assembly features and thermoplasticity in a pH-sensitive manner.[91] Similar to many other copolymers, suckerins are composed of repeating blocks of [Pro-M1-Pro-M2],[93] where M1 is rich in Ala and His, and M2 is abundant in glycine (Gly).[93,94] The M1 region assembles into a confined β-sheet structure stabilized by M2 composed of an amorphous matrix.[24a,93a,95] The histidine-containing M1 modules are pH- and temperature-responsive. At low pH, His residues can be protonated, thus the stability of β-sheet structures is diminished, resulting in the dissociation of β-sheet assemblies into random monomers at a lower temperature compared to in the neutral solution. Taking the A1H1 (AATAVSHTTHHA) (Table 1, Figure 6d) as an example, it is an amphiphilic peptide consisting of a hydrophobic head A1 (AATAVS) that is capable of driving β-sheet aggregation, and a hydrophilic tail H1 (HTTHHA) providing excellent solubility.[24] In addition to the formation of β-sheet-rich aggregates in water, A1H1 peptides can assemble into chiral nanostructures when exposed to polar solutions such as acetonitrile.[24a,c] A simulation study shows that below the transition temperature of aggregates (T_{agg}), A1H1 undergoes a transition from random-associated monomers into well-structured nanostructures due to primary and secondary nucleations followed by aggregated growth through elongation and coagulation.[91] The thermal hysteresis of A1H1 β-rich assemblies enables it to maintain the mechanical properties over a wide temperature range while allowing a pH-dependent release by reducing structural stability in acidic conditions.

3.1.2. Peptide–Polymer Hybrids

Synthetic polypeptides such as polymer–peptide hybrids are often generated using the ring-opening polymerization (ROP) of amino acid N-carboxyanhydrides (NCAs).[96] Typical examples including poly(ethylene glycol)–polypeptide copolymers (PEG-*b*-polypeptides) have been prepared through NCA polymerization using polymeric macroinitiators.[97] These synthetic peptide-based materials are able to assemble various secondary structures such as α helices, coils, and β sheets.[98] The selection of amino acids and their combinations offers diversity in sequence and structure. Thus, it can be used to manipulate the hydrophilic–lipophilic balances of polypeptides and allows the easier development of distinctive supramolecular structures compared to traditional synthetic monomers.[96a,98c,99]

Key strategies for preparing pH-responsive polymer–peptide hybrids and synthetic polypeptides can be summarized into four groups by manipulating i) ionization-induced, ii) pH-cleavable linkages, iii) pH-responsive shifts in secondary structure, and iv) supramolecular linkages as illustrated in **Figure 7**a.[97] The ionization-induced method employs the ionization in accordance with pK_a of amino acids as well as the response to the surrounding pH.[97] In general, these amino acids can be divided into two groups depending on the charge of their side chains (Figure 7b,c). His, Leu, and Arg are typical examples of amino acids with basic side chains while carrying a positive charge at a pH value below their pK_a. By contrast, Asp and Glu amino acids consisting of acidic carboxylic acid side chains carry negative charges at pH above their pK_a. Thus, pH-responsivity can be modified and manipulated by altering the choice of the amino acids with different ionizable functional groups in order to achieve the target hydrophilicity and physiochemical properties such as aggregation and assembly.

The second strategy is to manipulate the pH responsivity by attaching cleavable functional groups through pH-labile linkers, which are designed to be stable at physiological pH, but undergoes cleavage when exposed to acidic condition. The pH-labile linkers can be designed by selecting different pH-responsible components including amide,[100] anhydride,[101] hydrazone,[102] acetal,[103] imine,[104] and ketal.[105] Another design strategy for controlling the pH responsivity is by changing the secondary structure of polypeptides, for example, α helices, β sheets, and coils,[106] which depend on pH-responsive hydrophobic and ionic interactions. In exposure to pH changes, the secondary structure can switch from one form to another resulting in changes in structural rigidity, aggregation, and membrane permeability. Nevertheless, supramolecular with oppositely charged parts such as ionized amino acid residues, drug particles, and inorganic ions can be employed in designing pH-responsive peptide and protein systems. It mainly relies on noncovalent interactions, typically electrostatic and hydrophobic interactions between the charged side chains and the supramolecules. By altering the pH of their surroundings, it leads to the reduction in electrostatic forces that affect the characteristics of peptide- or protein-based materials.

A peptide-based ABA-triblock copolymer, poly(ʟ-lysine)-*b*-poly(propylene oxide)-*b*-poly(ʟ-lysine) (KPK) (Table 1) with high Lys weigh fractions of >75% exhibits pH-responsive conformational change from random coil to α-helix upon pH increase.[25]
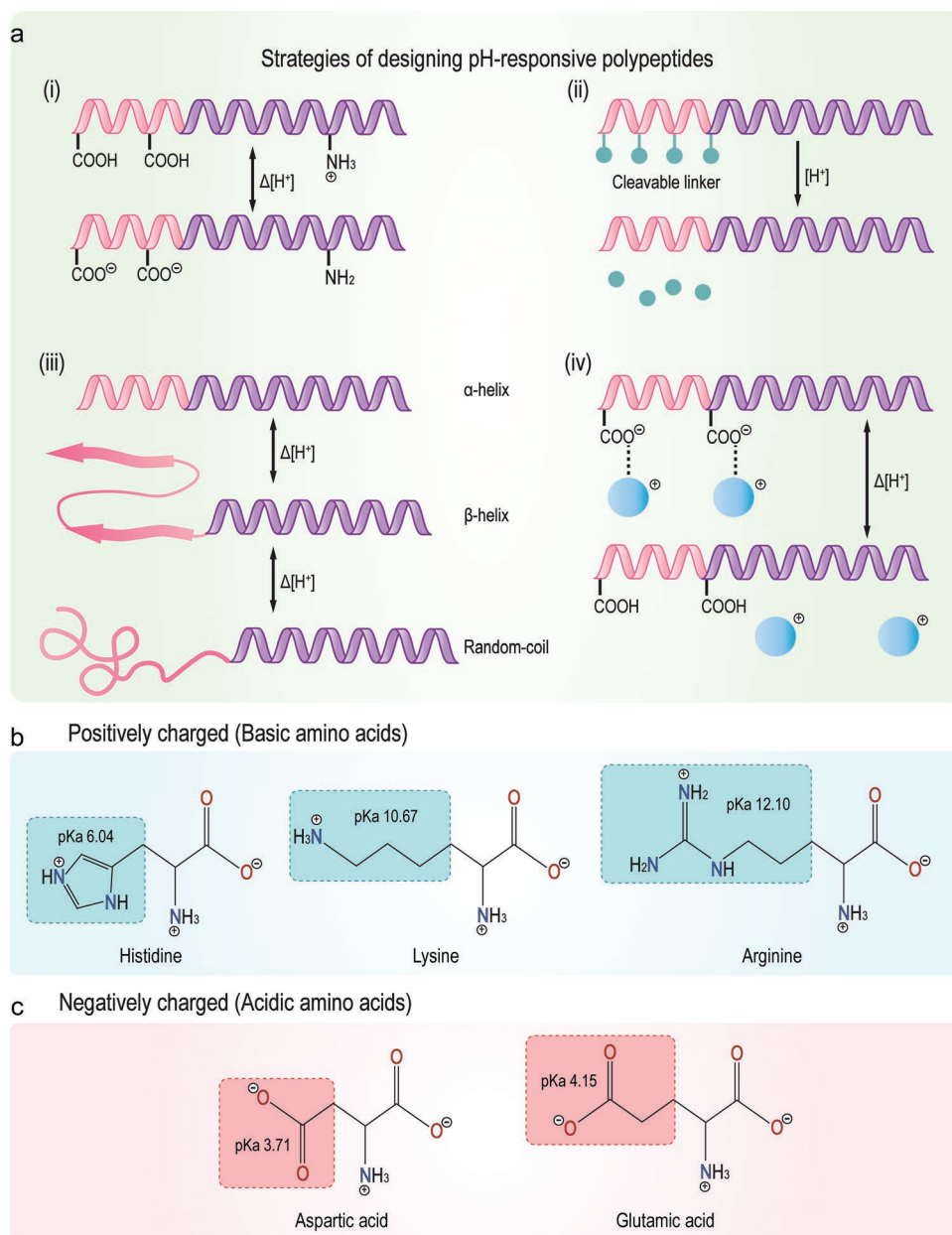
Figure 7. a) Design strategies of pH-responsive polypeptides and peptide–polymer hybrids including: (i) ionization induced, (ii) pH-cleavable linkages, (iii) change in secondary structure, and (iv) supramolecular. Structure of b) basic and c) acidic amino acids shown with pK_a values of their side chains.

As the pH is varied in the range of 3–7, spherical micelle-to-vesicles transform into spherical micelle-to-disk micelles dependent on the lengths of the K block. In general, Lys-based diblock copolymers increase their dimensions in solution when pH is decreased due to the ionic interactions and the protonation-triggered helix-coil transition of the K block. Consequently, an increase in aggregation size can be observed among PK diblock assemblies as the pH is reduced.[107] By contrast, the assembly size of the KPK triblock copolymer decreases as pH drops due to the sphere-vesicle morphology transition. In addition, the morphology transition is determined by the number of repeats in the KPK sequence. As pH increases, KPK 27 and 52 triblock amphiphiles exhibit spherical micelle-to-vesicle transi-

tions, while KPK 46 experiences a micelle-to-disk micelle transition as a result of decreased interfacial curvature.

3.1.3. Polypeptoids

Polypeptoids have been explored extensively due to their special structural characteristics and physiochemical properties.[97] Similar to polypeptides, polypeptoids exhibit low cytotoxicity, excellent biocompatibility, and can be modified with desirable properties.[108] It combines the features of naturally occurring macromolecules and synthetic molecules. In general, stimuli-responsive polypeptoids can be developed by connecting various

**ADVANCED
SCIENCE NEWS**

www.advancedsciencenews.com

**ADVANCED
FUNCTIONAL
MATERIALS**

www.afm-journal.de

functional groups to the nitrogen atoms on the backbone.[109] The interactions between hydrogen bonds and ions can be easily changed by adjusting the environmental pH, leading to a reversible microphase or reorganization.[110] Moreover, amino residues consisting of weak bases and acids can change their ionized states in accordance with pH.

Solid-phase submonomer synthesis (SPSS) and ROP have been employed to synthesize polypeptoids.[97] SPSS has been used in oligopeptides to offer precise control in polymer production. Various amine-containing reactive side chains can be introduced via displacement to achieve target stimuli-responsiveness.[111] In ROP, N-heterocyclic carbene and primary amines are often used to initiate the polymerization of polypeptoids from cyclic N-substituted N-carboxylic anhydride (NCA) monomers.[112] Other studies also show polypeptoids can be produced via N-substituted glycine N-thiocarboxylic anhydride (NTA) monomers using primary amine as the initiator.[113] To achieve the stimuli-sensitive activities, multicomponent reactions are introduced by using isocyanates, acids, aldehydes, and amines.[114] These polypeptoids can be designed into different structures such as homopolymer, random, draft, and block copolymer. The pH-responsive peptoid oligomers driven by sequence can also be produced by repeating bromoacylation and displacement in SPSS.[115] Secondary structure consisting of an ionizing group shows pH responsivity, for example, carboxylic acid of carboxyl phenylethyl. The embedded theory is based on the electrostatic interaction at different pH thus leading to the rearrangement of polymer structure.[116] By coupling the pH-triggered conformational shifts with fluorescence intensity variations, it offers potential applications in biocompatible pH sensors.[117] Other applications have also been reviewed, such as antifouling surface coating.[118] A systematic review has been published by Fang et al.,[4a] so we will not further discuss it in this review.

3.2. Applications

A wide variety of pH responsive biomolecules have been designed for various targeted delivery applications taking advantage of the acidic extracellular microenvironment (pH 6.4–6.8) or acidic intracellular organelles (e.g., pH 4–6.5 for endosome or lysosome) in tumors compared to the normal physiological pH of 7.4.[119] A tumor specific pH responsive peptide (RK(HHHHHHH)RR, $H_7K(R_2)_2$) was designed based on a arginine-rich cell penetrating peptide. The R-rich sequence with a branched structure has a stronger cell penetrating activity than that with a linear structure. The polyhistidine (H_7) is able to respond to the acidic tumor microenvironment. Then the $H_7K(R_2)_2$ was conjugated to a diblock copolymer PLGA–PEG (Table 1), and it formed polymeric micelles loaded with paclitaxel (PTX-PM-$H_7K(R_2)_2$). During blood circulation with a pH 7.4, the H_7 is mainly located at the interface of the hydrophobic PLGA core while the $(R_2)_2$ resides in the hydrophilic PEG shell. When the polymeric micelles arrive at the tumor sites with a lower pH, the H_7 is protonated making it more hydrophilic, thus exposing $(R_2)_2$ from the PEG shell, which makes it available to facilitate the cell penetration. Although many pH responsive polymeric micelles have been developed, this $H_7K(R_2)_2$ modi-

fied micelle offers a new strategy for pH triggered cell penetration for tumor targeted delivery.[26] Also, Zhao et al. developed $H_7K(R_2)_2$-modified pH-sensitive liposomes loaded with doxorubicin for targeted glioma drug delivery, showing pH triggered specific targeting effect in both rat C6 glioma tumor model and U87-MC orthotopic tumor model.[120]

Similarly, an R_6H_4 (RRRRRRHHHH) peptide has a pH responsive cell-penetrating property. Together with an active targeting ligand hyaluronic acid (HA), a dual-functional liposome was constructed for tumor targeted delivery. PTX loaded HA-R6H4 liposomes showed strong antitumor efficacy using murine hepatic tumor models.[121] In addition, Moyer et al. designed two pH responsive amphiphile peptides (PA1 and PA2) which self-assemble into nanostructures with distinct morphology.[27] PA1 contains H_6, palmitic acid as a hydrophobic tail at the N-terminus, and an oligo(ethylene glycol) (OEG) at the C-terminus to improve solubility. PA1 (Table 1) self-assembles into nanofibers at pH 7.5 due to the pH sensitive β-sheet forming peptide H_6, while below pH 6.5 it disassembles because of the positive charge repulsion from the protonated His. By contrast, PA2 (Table 1) was designed with the C and N termini of PA1 switched, leading to its assembly into a spherical structure having a core with a radius of 0.95 nm and a shell thickness of 2.8 nm. Interestingly, the pH-responsive PA1 nanofibers showed enhanced tumor accumulation compared to spherical micelles as well as nonresponsive nanofibers, demonstrating a promising approach to improve the pharmacological properties of nanomedicines. Additionally, poly(L-lysine), a cationic biopolymer, has been widely studied as a pH-responsive system for gene therapy, drug delivery, nanoelectronics, and sensing.[122]

pH-responsive hydrogels have been widely studied for various applications in recent years. Schneider and co-workers designed a pH-dependent hydrogel MAX 1 (Table 1) that can self-assemble and form hydrogel.[28] At low pH, these peptides remain unstructured with a low viscosity. As pH increases to pH 9, they self-assemble into an amphiphilic β-hairpin structure due to intramolecular folding and then form a rigid but shear-thinning hydrogel. A modified MAX8 by replacing the second Lys in the sequence (PPTKVK) to Glu, it can be used as an injectable hydrogel for localized curcumin delivery.[123] Zhang et al. reported a self-assembled dipeptide derivative, ferrocene-diphenylalanine (Fc-FF) (Table 1), that is able to form ultra-pH-sensitive hydrogel.[29] At pH above 5.9, (L)-Fc-FFs self-assemble into nanospheres with a diameter of 200–400 nm. Their structure shifts to nanohelices at pH 5.7–5.9 and form rigid nanobelts as pH reduces to 5.5. In addition, using a mixture of (L)-Fc-FF and (D)-Fc-FF enables the formation of stable hydrogels at a lower pH. This study reveals that the gelation and subsequent hydrogel properties such as rigidity and strength can be manipulated by changing the chirality of peptides under different pH. Novelli et al. designed a peptide amphiphile lauroyl-Gly-Gly-D-Ser-D-Lys-NH$_2$ trifluoroacetic acid (C12-GCSK) (Table 1).[30] It self-assembles into spherical micelles at acidic pH (**Figure 8**a), but forms self-aggregates and reshapes toward fibers at basic pH as a result of its conformational transition from random coil to β-sheet. Carlini et al. reported modified KLD-12 peptide (Table 1) for pH-sensitive hydrogels based on charge-conversion.[31] Self-assembling
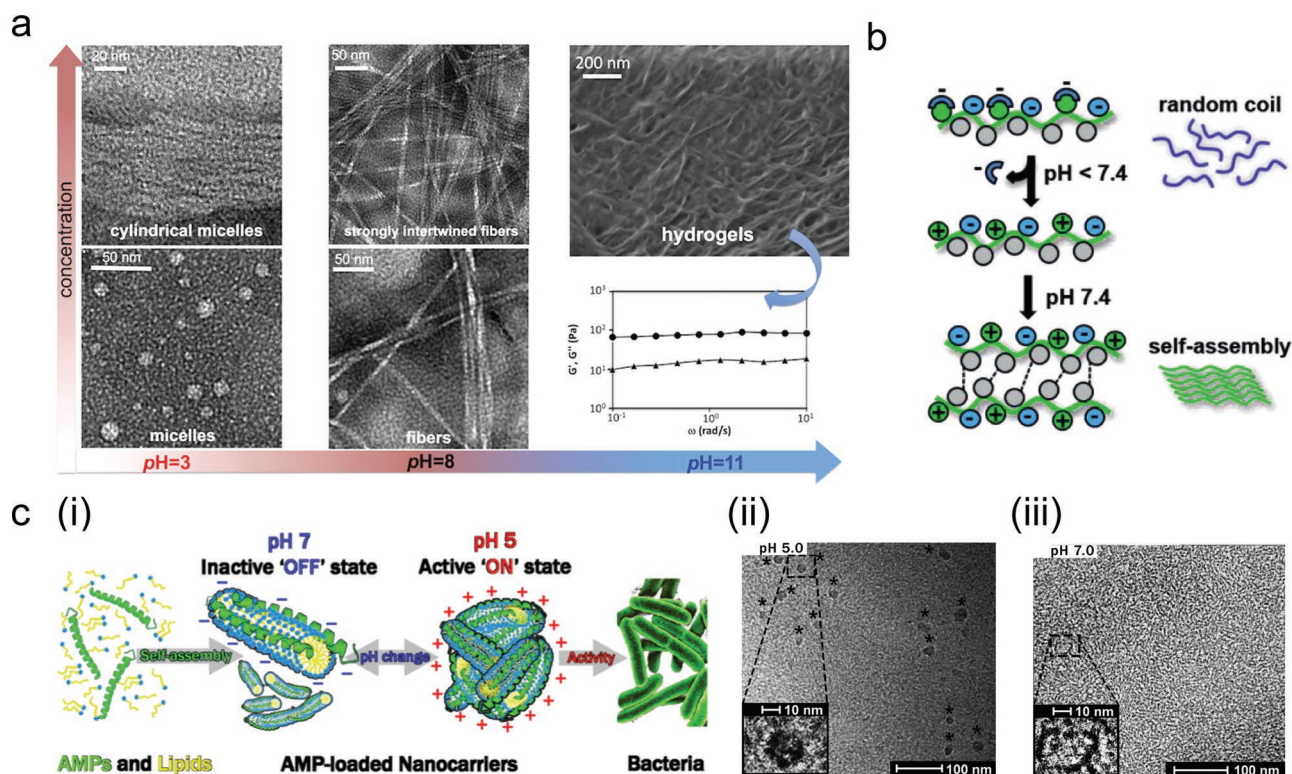
Figure 8. a) TEM images of C12-GCSK peptides self-assemble into different structures upon the change of concentration and pH. Reproduced with permission.[30] Copyright 2020, American Chemical Society. b) Illustration of polyanionic charge-conversion peptides KLD undergo conformational change from random coil to β-sheet at pH 7.4. Reproduced with permission.[31] Copyright 2021, Wiley-VCH. c) (i) Scheme of pH-switchable antimicrobial nano-self-assemblies between pH 5 and 7; cryo-TEM images of LL-37/OA nano dispersion in the PBS at pH 5 (ii) when polydisperse particles with average diameter of 14.9 ± 6.1 nm and at pH 7 (iii) when forming branched cylindrical micelles with cross-sectional diameter of 5.0 nm. Reproduced with permission.[125] Copyright 2018, American Chemical Society.

peptide KLD-12 forms degradable, nonimmunogenic and nontoxic hydrogel.[124] However, its practical applications for traumatic injury using catheter delivery is limited due to its high viscosity. The modified KLD-12 biomolecules consist of maleic acid (mal-KLD), citraconic acid (cit-KLD), or dimethylmaleic acid amide (dma-KLD) masking group on the Lys residues. So acid-trigged Lys unmasking induces their self-assembly into β-sheets due to the cross-linking and hydrophobic interactions at pH lower than 7.4 (Figure 8b). When injured, these peptides form various scale gelation at impacted tissue acidosis and remain assembled at neutral pH. This dynamic structure-shifting behavior is attractive for wound-healing and inflammation-associated applications.

pH-responsive antimicrobial peptides (AMPs) have also attracted interests. Gontsarik et al. designed and characterized a pH-sensitive amphiphilic biomaterial with antibacterial activity through the self-assembly of oleic acid (OA) and human cathelicidin (LL-37).[125] Core–shell cylindrical micelles were formed at pH 7 with a diameter of 5.5 nm and a length of 23 nm. These micelles undergone a colloidal transformation at pH 5 to form branched threadlike micelles aggregates (Figure 8c). The cationic LL-37/OA aggregates showed strong antimicrobial activity at pH 5, while it lost the activity upon increasing the pH to 7. The switch "on" and "off" in response to changes in pH enables the targeted peptide delivery to tissues with abnormal pH while minimizing activity at the healthy sites, thus reduces the side effects.[126]

4. Light-Responsive Biomolecules

Light has attracted huge attention as a trigger due to its spatial and temporal modulated operation and localization.[127] Most nature proteins are affected by photon absorption contributing to biological catalysts, information and energy traffickers.[3] For example, rhodopsin is a light-sensitive protein enabling vision in dark conditions. It is the most sensitive at 498 nm when the photopigment is in rod morphology.[128] Inspired by these naturally existing peptides and proteins, light-responsive biomolecules have emerged as a novel class of photoswitchable materials.

4.1. Design Principles

Photosensitive systems are advantageous due to their simple activation mode as neither chemical catalysts nor exogenous components are needed.[129] Recent innovations in the fields of optochemical genetics and photopharmacology lead to the development of novel light-responsive molecules that are capable of switching from "bioactive" to "inactive" state upon exposure to their specific wavelength-sensitive range.[127b,130] The combination of photochromic molecules such as azobenzenes (Azos), spiropyrans, and diarylethenes with biomolecules extends the scope of stimuli-responsive materials and has been extensively studied.[127b]

Many photochromic molecules respond to light by forming or breaking bonds that triggers shifts in polarity and geometry.[127a,131] However, increased degree of freedom in states leads to reduction in conformational control. By comparison, molecules acting as photoswitches that are switchable between E and Z double bonds provide more predictable and controllable structural properties.[127a] Among these molecules, isomerization is often triggered by photon adsorption to enable an electron-excited state, thus reducing the energy barrier between E and Z states. Decay to the electronic ground state restores the energy gap, and traps the thermally unstable isomer. The current energy state and the value of energy barriers manipulate the relaxation rate to a more thermodynamically stable isomer. Compared to stilbenes,[132] hemithioindigos,[133] thioxopeptides,[134] selenoxopeptides,[135] diarylethenes,[136] acylhydrazones,[137] and rhodopsin-like molecules[137] as photoswitches, Azos[138] currently give the widest range of excitation wavelengths and stability of photoactivated states. The detailed design of azophotocontrol peptides and proteins has been reviewed by Mart and Allemann in 2016.[127a]

α-helix has been used as a basic structure in designing light-sensitive peptides and proteins. Photomechanical changes can be induced in light-responsive systems when exposed to a specific wavelength of light. Photoresponsivity of the biomolecules is normally induced by E–Z isomerization, degradation led by bonds or linkers cleavage, or dimerization. The majority of the photoswitchable systems regard the Azos as the chromophoric linkers. A typical example is (3,3′-bis(sulfonato)-4,4′-bis(chloroacetamide)azobenzene (BSBCA), isomerization of the central double bond can be shifted between the E- and Z- conformers upon illumination.[3] It is attractive since the isomerization is highly reversible, with a high quantum yield and not sensitive to other environmental factors. Nevertheless, the intracellular environment might constrain their applications as they are sensitive to reducing agents.

Photoswitches can be easily linked to biomolecules by targeting the thiol group of cysteine (Cys) residues.[127b] The Cys side chains located on the surface react readily with para-haloacetamide substituted Azos.[127a] Previous work indicated that with Cys pairs in i, $i + 4$, or $i + 7$ spacings along the peptide chain, the α-helical structure is stabilized by the Z-isomer of iodoacetamidoazobenzene while with pairs of Cys pairs in i, $i + 11$ spacings α-helical structure is stabilized by E-isomer.[127a] The water-soluble Azo expanded the scope of light-sensitive applications by allowing controlled protein–protein, DNA–protein, and RNA–protein interactions via α-helical motifs.[139] Recently, novel photochromic molecules which can be activated by higher wavelengths have been developed offering photoswitchable behaviors upon exposure to nontoxic visible light in a range of 370–550 nm in water.[140]

4.1.1. Peptides

Photoresponsive bicyclic peptides have been synthesized for potential applications in many synthetic bicyclic peptides containing 2–5 amino acids in loops.[127] Bicyclic peptides are valuable molecular scaffolds for the development of potent ligands for various protein targets. In order to create n cycles in a peptide, $n + 1$ points need to be linked via a linchpin with $n + 1$ reactive functionality. For instance, dibromomethyl benzene (DBMB) and tribromomethyl benzene (TBMB) are C2v and C3v symmetrical linchpins for turning linear unprotected peptide chain consisting of 2–3 Cys residues into monocyclic and bicyclic peptides.[127b] The incorporation of two Azb molecules in a linchpin is not ideal, as they isomerize independently, resulting in a poor light-responsive performance. However, the use of a non-C3$_V$ symmetric linchpin consisting of the exact same three reactive groups is impractical, because its reaction with a peptide produces three or more isomers. A feasible approach for synthesizing such light responsive bicycles is to use a C2v symmetric linchpin having 2 + 1 functional groups that target at 2 and 1 orthogonal functionalities in a single peptide. An alternative method is to redesign static bidentate C2v symmetric lynchpins into C2v linchpins consisting of light-responsive components such as azodicarbonamide by employing BSBCA to construct light-responsive macrocycles (**Figure 9**a).[127b,139b,141] An Azo (HADCAz) LR-linker containing tridentate C2-symmetric hydroxyl amine and dichlorobenzene was developed with two reactive groups chlorobenzyl and hydroxylamine, which enable the conversion from a linear unprotected peptide into a bicyclic peptide via a one-pot, two-step reaction. The linker is capable of undergoing a reversible isomerization from E- to Z upon irradiation at 365 nm. Therefore, this bicyclic peptide consisting of two loops of amino acids is capable of conformation change responding to visible light.

4.1.2. Proteins

Photosensitive protein fibers have been developed with reversibly modulated mechanical stiffness and toughness[32] by assembling a positively supercharged polypeptide (SUP) with negatively charged surface-active modules consisting of Azo molecules via electrostatic interactions. The reversible E–Z isomerization of Azo alters the packing of the local intermolecular environment and changes cation–π interactions, thus enabling the modulation of noncovalently assembled structures and consequently the mechanical properties of the formed fibers. The pentapeptide repeat unit $(VPGKG)_n$ consisting of Lys at the fourth position gives a high net charge for SUPs (Figure 9b). The conformational rearrangement of the Azo units induced by isomerization leads to changes in the interactions between the free cationic Lys residue of neighboring SUP–Azo compounds (Table 1) and Azo phenyl rings. The mechanical property of the SUP–Azo fibers increases due to the conformational shift from E- to Z-state in the solid state, because the strength of cation–π interaction is increased in its Z-state. Furthermore, the mechanical properties of the fibers can be restored when the isomerization state is changed back to E-state. This attempt offers a novel design pathway for designing protein-based biocompatible smart materials.

A genetically encoded light-responsive protein-based polymer was designed by incorporating photoswitchable unnatural amino acids (uAAs) at multiple sites (Table 1).[33] Recombinant fusion has been widely investigated to develop fusion proteins with desired functions and properties that can be achieved by recombinantly fusing light-sensitive sequences
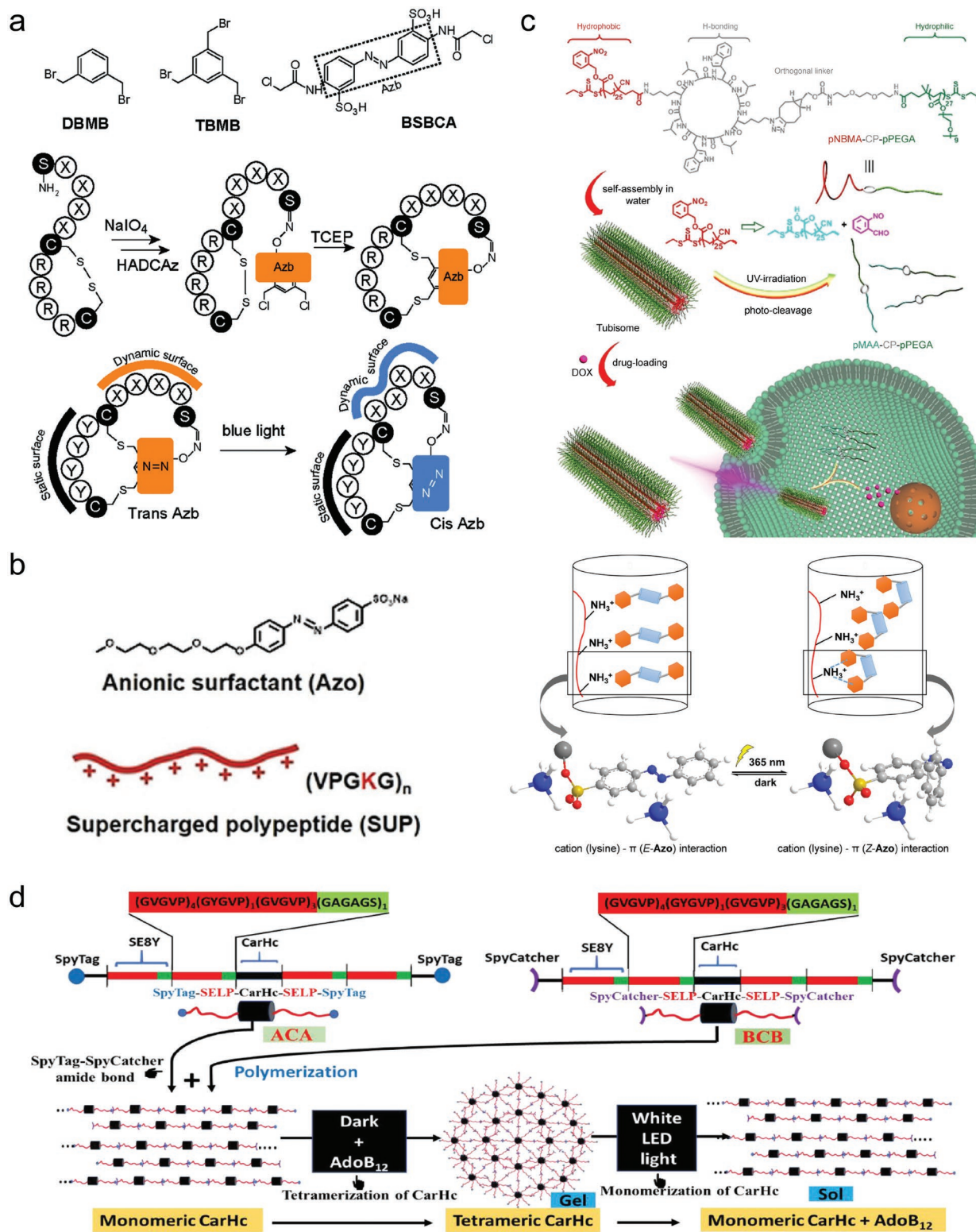
Figure 9. a) Linchpins and strategies used for synthesizing cyclic and bicyclic biomolecules with static or dynamic surfaces. Thiol-targeting linchpins are adopted for the production of monocyclic (DBMB), bicyclic (TBMB), and monocyclic (BSBCA) LR-peptides. Reproduced with permission.[127b] Copyright 2018, Royal Society of Chemistry. b) Illustration (left) of the photoresponsive SUP-Azo assembled of cationic K108cys (SUP) and anionic Azo surfactant. Schematic representation (right) of the mechanism of photoswitchable SUP-Azo fibers. Reproduced with permission.[32] Copyright 2020, Wiley-VCH. c) Illustration of cellular uptake of DOX-loaded tubisomes and phototriggered intracellular drug release. Reproduced with permission.[142] Copyright 2020, Wiley-VCH. d) Schematic diagram of the assembled structure of recombinant SELPs incorporated with photoresponsive CarHc peptide. Reproduced with permission.[129] Copyright 2020, Elsevier.

**ADVANCED
SCIENCE NEWS**

www.advancedsciencenews.com

**ADVANCED
FUNCTIONAL
MATERIALS**

www.afm-journal.de

or domains to a target protein.[129,143] However, the fusion may affect the functions of the target biomolecule and constrain the types of light-sensitive properties. Alternatively, photoswitchable small molecules can be incorporated into proteins by attaching them to an uncovered peptide backbone or a reactive side chain,[144] but this approach is limited by the efficiency of the conjugation chemistries due to the constrained accessible sites of small peptides. Therefore, a better strategy was proposed to enable the fine-tuning of light-responsive properties of biomolecule-based materials by positioning small-size light-sensitive sequences in the primary structure of the polypeptide. The development of novel chromosomal aminoacyl-tRNA synthetases (aaRSs) for Azo-bearing uAAs yielded a 40-fold higher protein production. This novel approach offers a new design pathway for constructing tailored and tunable photoresponsive proteins.

4.2. Applications

Light-responsive materials have been extensively explored due to their capabilities in high spatiotemporal control in a noninvasive fashion.[32] This class of materials normally incorporate a light sensitive ligand such as Azo with a functional peptide or protein sequence. Several examples will be touched on to give a broader understanding toward the light-induced applications such as targeted drug and DNA delivery, controlled release, biomimetic devices, and soft robotics.

Light-sensitive tubisomes were synthesized based on a cyclic peptide-bridged amphiphilic block copolymer (CPA) (Table 1, Figure 9c).[142] It consists of a hydrophilic part, poly-PEG acrylate (pPEGA), and a hydrophobic and photoresponsive polymer, poly-2-nitrobenzyl methacrylate (pNBMA), conjugated to the opposite side of the cyclic peptide. The well-defined hydrophilic polymers pPEGA and photosensitive polymer pNBMA were synthesized respectively using the reversible addition–fragmentation chain transfer polymerization.[145] Driven by the hydrophobic interactions and hydrogen bonding, CPA hierarchical tubisomes were formed in liquids. Exposure of the self-assembled particles to UV irradiation (365 nm) triggered the hydrophobic-to-hydrophilic transition resulting in the disassembly of the CPA tubisomes. Moreover, these tubisomes demonstrated great potential as biocompatible drug delivery.

Dynamically light-responsive biomaterials are attractive for biomedical applications such as biomimetic devices and soft robotics.[129] A photosensitive silk-elastin-like protein (SELP)-CarHc hydrogel (Figure 9d) was synthesized via SpyTag-Spy-Catcher chemistry. AdoB12-dependent CarHc tetramerization was identified as the essential step in forming hydrogel in dark. Under exposure to white light, the gel softens due to the dissociation of a molecular network as a result of the conversion of CarHc tetramer back to monomers. A photocaged dehydropeptide (CNB-Phe-ΔPhe-OH) was reported capable of forming a stimuli-responsive supramolecular hydrogel.[146] It consists of a UV-cleavable carboxy-2-nitrobenzyl (CNB) group. The pendant aromatic capping group is cleaved to free the corresponding uncaged model dehydropeptide (H-Phe-ΔPhe-OH) upon exposure to UV light, thus enabling the dissolution of the hydrogel

due to the disturbance of intramolecular interactions. This feature allows the hydrogel to disassemble in a noninvasive manner with spatial and temporal control that provides possibilities for unique demand-driven drug release, wound healing materials, and other potential treatments.

Yin et al. reported light-responsive helical peptides for DNA delivery.[34] The developed cationic peptide named PVBLG-8 has high molecular weight, α-helical structure, and is capable of cell-penetrating. Due to the large molecular weight and high charge density, PVBLG-8 offers a more effective DNA delivery in mammalian cells which can serve as a good vector for gene delivery.[147] However, the designed peptides shows cytotoxicity at high concentration and provides little DNA release due to their high cationic charge. A modified PDMNBLG-r-PVBLG-8 (Table 1) was developed with α-helical structure by reducing the charge density and helical content at post-transfection state. By incorporating the light-sensitive 4,5-dimethoxy-2-nitrobenzyl-glutamate (DMNBLG), these peptides provide efficient membrane activity during the transfection and transform to a less toxic and DNA-repelling state due to the disruption of helical structure and cationic charge reduction upon UV (346 nm) or NIR (750 nm) exposure (**Figure 10**a).

Morales et al. reported a near-infrared (800 nm) triggered nanocarriers for controlled release of the toxic α-helical amphipathic peptide $(KLAKLAK)_2$ that can be used to disrupt the membrane of mitochondrial cells.[148] A poly-His variant $(KLAKLAK)_2$ peptides (H_6PAD) were bonded to a nitrilotriacetic acid (NTA) in the presence of nickel due to the affinity of His tags to NTA. Then a streptavidin (STV) labeled with cell-penetrating peptides TAT (YGRKKRRQRRRPQ) was conjugated to the NTA-H_6PAD. The designed functional sequence was then linked to DNA-bonded hollow gold nanoshells leaving the STV–TAT facing out. Upon exposure to NIR light, the cleavage of thiol–gold bond enables the peptide release and breaches the endosome membrane for cytosolic activity (Figure 10b).

5. Metal Ion-Responsive Biomolecules

In nature, metals play important roles due to their catalyzing ability involved in many processes such as photosynthesis and redox reactions.[3,149] Approximately one-third of enzymes require metallic cofactors to achieve specific functions.[150] Many peptides, for instance, can self-assemble into nanostructures including nanofibers, nanotubes, and helical ribbons via metal–ligand interactions.[151] Metal ions also contribute to the structural, regulatory, and enzymatic features of peptides and proteins. For example, the zinc finger motif is a protein structure stabilized by the coordination of zinc ions. For decades, great efforts have been made into synthesizing artificial biomolecules that can mimic naturally occurring metallopeptides with natural or artificial metal-binding sites.[152] In addition, peptide–metal coordination is capable of inducing conformational changes in the biomolecular structure, thus resulting in significant changes in properties and functions.[153] For example, Alzheimer's disease is normally triggered by the transition from α-helix or β-sheet to β-amyloid via coordination with metal ions.[154]
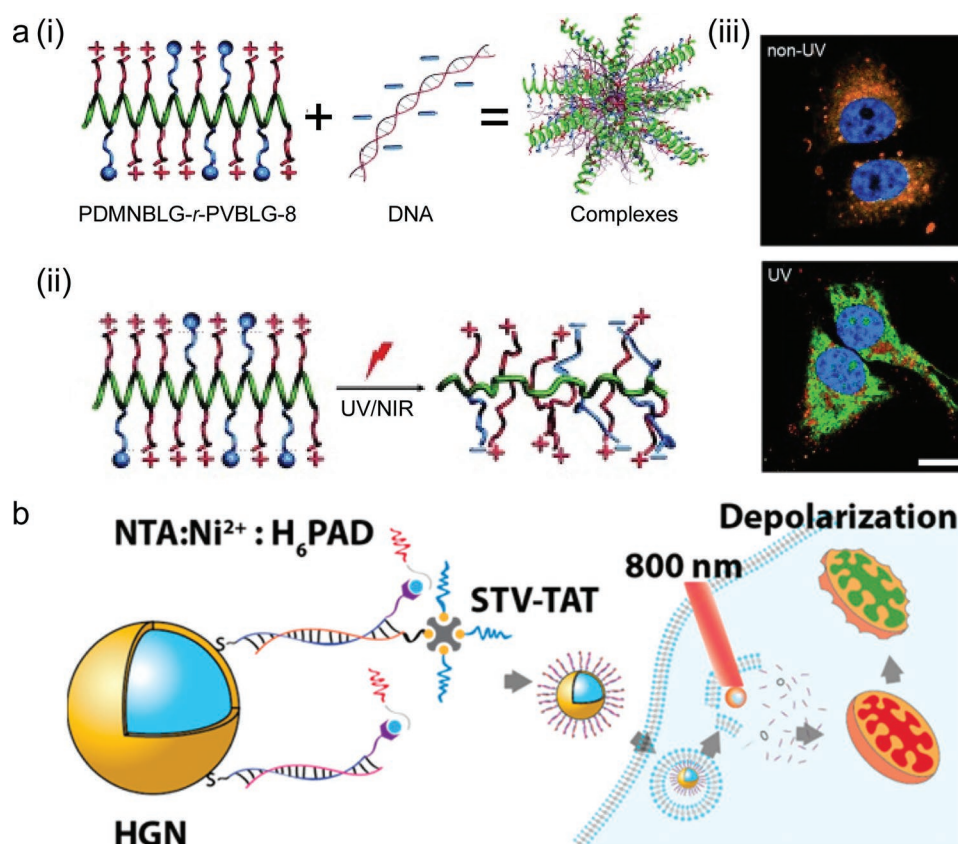
Figure 10. a) (i) Schematic diagram of PDMNBLG-r-PVBLG-8/DNA complex formation. (ii) Light-initiated conformational change. (iii) Confocal images of HeLa cells cultured with RhB-P20 in red and YOYO-1-DNA in green before and after UV treatment (bar represents 20 µm). Reproduced with permission.[34] Copyright 2013, Wiley-VCH. b) Light-triggered peptide release using nanocarriers HGN-MPC. Reproduced with permission.[148] Copyright 2017, American Chemical Society.

5.1. Design Principles

Commonly used functional groups that undergo metal-induced self-assembly are important in designing peptide building blocks.[149] His,[155] Cys,[156] Trp,[155h] and Glu[157] are natural ligands that form metal–ligand coordinating bonds with various metal ions such as Zn^{2+}, Cd^{2+}, Cu^{2+}, Ni^{2+}, Ag^+, Hg^{2+}, Pb^2, La^{3+}, Yb^{3+}, Ca^{2+} Ti^{4+}, Mo^{6+}, etc. Their interactions with metals induce conformational alternations or generate supramolecular structures. For example, His consists of an imidazole functional group bearing a nitrogen lone pair that is capable of interacting with metal ions. This makes His often used in controlling the structure of metal–organic structures, thus enabling their stimuli-responsive properties. The AM1 peptide designed according to a naturally existing peptide Lac21 is metal ion-responsive.[17a] In the presence of zinc ions, a stable foam can be formed due to the ion coordination bonding formed between His amino residues and zinc ions, it can be switched off by using a chelating agent such as EDTA.

By contrast, artificial peptides have been designed by incorporating various metal-ion responsive ligands to tune material properties.[158] In particular, these peptide molecules have not only metal–ligand coordination but also specific binding ability.[159] The specific binding motif exploits the coordination bond and contributes to precise control of the structural stability and strength of the assembled materials.[160] Artificial ligands such as pyridine, iminodiacetate, etc., are widely investigated and have been comprehensively reviewed.[149]

5.2. Applications

5.2.1. Calcium

Calcium ions have been frequently used in designing stimuli-responsive peptides and proteins. The repeat-in-toxin (RTX) motif of *Adenylate cyclase* from *Bordetella pertussis* has been investigated for calcium-sensitive hydrogel assembly.[35a,161] This intrinsically disordered peptide is able to fold into a β-roll structure in the presence of calcium ions.[162] Incorporating a capping group at the C-terminal of this peptide is essential for the folding as well as the switch between the folded and unfolded structure with or without calcium ions,[163] while the wild-type peptide does not exhibit this self-assembly property.[163d,164] Two mutants, namely, DLeu β-roll and 406 β-roll (Table 1), were designed. They both responded to calcium with similar affinities of 0.9–1.2 mM as the wild type β-roll. For the DLeu, all the amino residues located at the β-roll faces were replaced with Leu. Driven by the hydrophobic force exerted by the Leu amino residues, these peptides can self-assemble into hydrogels.[35b,161]

By contrast, the mutant 406 was modified to specifically bind to lysozyme controlled by calcium concentrations.[35b,161] A bifunctional calcium-sensitive hydrogel by combining DLeu and 406 motifs, maltose-binding protein (MBP)-DLeu-406-406-DLeu, was constructed that can bind to lysozymes at the protein surface and capture the targets in the assembled structure. Moreover, the oligomerization and target-binding properties can be manipulated by calcium concentration. The monomeric hydrogel building block is constructed by MBP aiding to express and purify hydrogel. In addition, the scope of hydrogel construction is further extended by replacing the concatemer of 406 β-roll with other functional peptide sequences or different β-roll mutants. This inspires innovations toward target release and controllable self-assembly.

A β-roll peptide has been designed for biomolecular recognition (**Figure 11**a).[35b] Similarly, incorporation of several repeats of the RTX domain makes it form a β-roll structure upon calcium binding, but remains unstructured without calcium ions.[165] Multiple Gly and Asp amino acids in their sequence

contribute to structural flexibility and calcium-binding.[164b,d,166] It undergoes a polarized conformation transition by increasing the extracellular calcium concentration (> 0.1 mM).[163a,165c,166,167] This peptide provides a novel calcium-responsive scaffold that can be adopted for target molecular recognition and self-assembly.

5.2.2. Sodium

Salt ions can interact with charged AA side chains and thus can be used to manipulate the secondary structure of biomolecules. Yuan et al. reported a helix–coil transition of ionic polypeptides triggered by salt and pH under physiological conditions.[36] A series of ethylene glycol (EG$_x$)-linked polypeptide electrolytes were functionalized with tertiary amine groups resulting in pH and salt-mediated secondary structure changes. For example, the P(EG$_x$DMA-Glu)$_{50}$ (Table 1, Figure 11b) remains unfolded in acidic conditions but undergoes a salt-triggered coil-to-helix
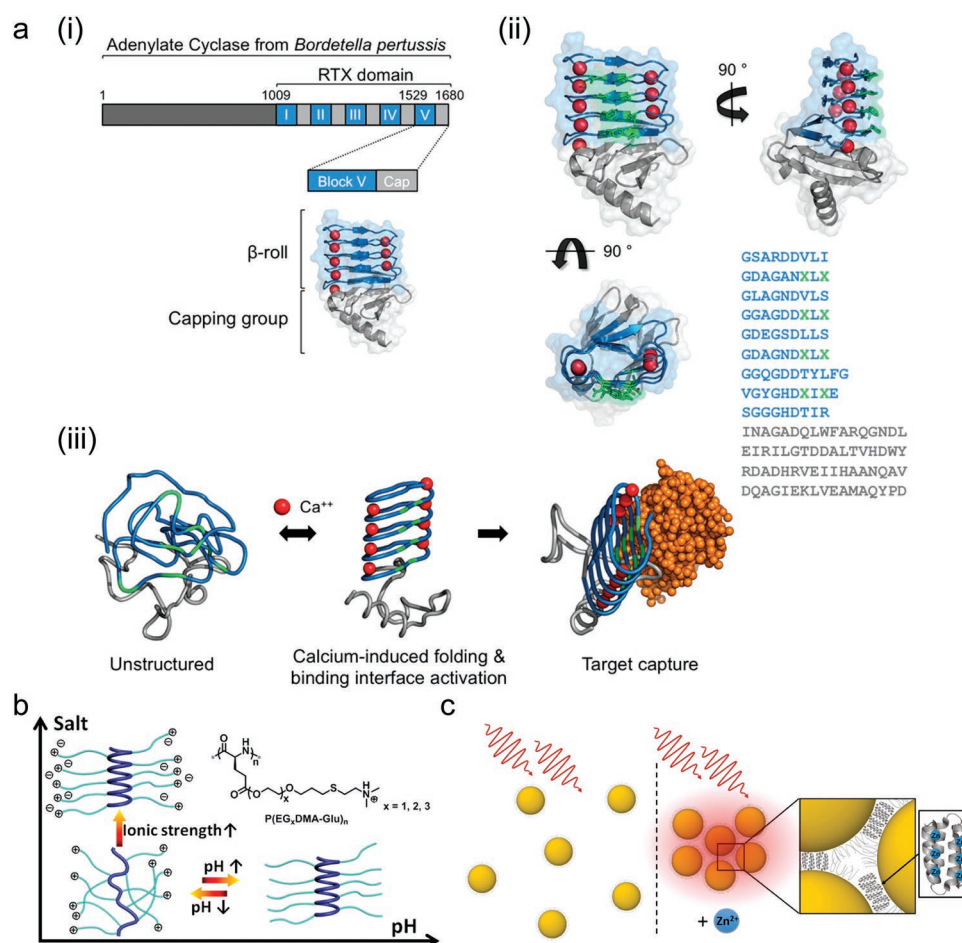

Figure 11. a) Schematic diagram of the β-roll peptide with a capping group. (i) Adenylate cyclase enzyme consists of five repeats of RTX domains. (ii) Peptide sequence and tertiary structure at different orientations. Eight amino residues are highlighted in green showing the β-roll face. (iii) Demonstration of the calcium-induced shift in structure. The unstructured polypeptide transforms to a β-roll structure upon the addition of Ca^{2+} ions, resulting in the binding of the target capture (in orange) and polypeptide interface (in green). Reproduced with permission.[35] Copyright 2017, American Chemical Society. b) Illustration of the pH- and salt-triggered transition in the structure of P(EG$_x$DMA-Glu). Reproduced with permission.[36] Copyright 2018, American Chemical Society. c) Diagrammatic representation of spherical Au NPs with a diameter of 20 nm functionalized by JR2EC undergo a dispersed-to-aggregated state transition upon the addition of zinc ions. Reproduced with permission.[37] Copyright 2017, American Chemical Society.

**ADVANCED
SCIENCE NEWS**

www.advancedsciencenews.com

**ADVANCED
FUNCTIONAL
MATERIALS**

www.afm-journal.de

structural shift and reaches maximum helicities at the NaCl concentration of 120 mm driven by protonation. This work highlights salt-based stimuli-responsive conformation changes of polypeptides by incorporating a fine-tuning linker representing a facile approach to designing smart materials.

5.2.3. Zinc

Zinc ions play a significant role in biomedical processes including carcinogenesis,[168] neural signaling,[169] etc. A zinc- and protease-(MMP-7) sensitive polypeptide JR2EC (Table 1, Figure 11c) was designed and produced using an automated peptide synthesizer. It can be used as an ion-induced contrast medium demonstrating multiphoton-triggered luminescence. JR2EC polypeptides form a helix–loop–helix structure and homodimerize into four-helix bundles in the presence of 5 mm Zn^{2+}. Upon homodimerization, the polypeptides immobilized on the well-dispersed Au NPs can form extensive aggregation. In addition, this process can be reversed by complexation of Zn^{2+} by EDTA. By adding Zn^{2+} or EDTA in excess, the signal of multiphoton-induced luminescence could be reversibly switched on or off, correspondingly. The two recognition sites located on JR2EC enable them to bind with MMP-7, which could be potentially used for investigating cancer progression and tissue inflammation.

5.2.4. Other Ions

Silver has been studied for prophylactic treatment of infections.[170] A histidine-based aliphatic peptide IH6 (Table 1) was designed to immobilize the Ag^+ via coordination bonding between His and Ag^+.[38] Upon silver ions addition the IH6 undergoes a conformational shift from antiparallel to parallel β-sheet (**Figure 12**a) thus forming a hydrogel, which allows the controlled release of silver ions, thus enabling a sustained antibacterial effect. D'Souza et al. designed a short peptide, L9 (Table 1) with nine amino acids that can self-assemble into organized structure upon silver addition.[39] Incorporating an unnatural amino acid 3'-pyridyl alanine (3'-PyA) at both ends of the peptide sequence (LRLRLRL) contributes to the interaction with silver and gelation at neutral pH. L9 consists of an antibacterial LRLRLRL part due to the binding of the positively charged Arg to the negatively charged bacterial membrane. By adding Ag^+ (1.88 mm), L9 self-assembles into a β-sheet structure, then a strong hydrogel. In vitro study showed Ag-L9-based hydrogel killed *E. coli* and *Staphylococcus aureus* without affecting fibroblasts. This hydrogel has potential for injectable, antimicrobial wound dressing.

Copper has been identified as an important indicator for Alzheimer's disease (AD) progression, as the aggregation of copper and Aβ is the main feature of AD. Zhang et al. developed a Cu-binding sequence consisting of SAQIAPH (PCu) using phage display for inhibition of amyloid β peptide (Aβ) aggregation.[171] In vitro experiments using N2a-sw cells showed a significant reduction in the formation of amorphous and granular aggregates in the presence of PCu compared to the negative control (Figure 12b). The biocompatibility of PCu

and its efficiency to ameliorate the toxicity of cupper ions was studied at different copper ion concentrations (10, 30, 50, 70, and 90 μm). The cell viability was significantly reduced to below 50% when incubating with cooper of 90 μm. By contrast, the cell viability remained at 100% when coincubated with 100 μm PCu. Feng et al. reported a stimuli-responsive nanoindicator for copper ion imaging.[40] A borono-peptide, B(OH)$_2$FFFRGD-OH (BP) (Table 1), was constructed as a fluorescent probe for Cu (II) detection. It is capable of self-assembling into nanofibers driven by intermolecular forces. These nanostructures bind to alizarin red S (ARS) and produce a spherical nanoindicator with strong fluorescent signal, while the fluorescence could be quenched upon adding copper ions due to the displacement effect and formation of ARS/Cu (II) complex. A range of copper ion concentrations of 0–16 μm was used showing a dose-dependent fluorescence behavior (Figure 12c).

6. Enzyme-Responsive Biomolecules

Enzyme plays critical roles in biorecognition and catalysis in living organisms. The presence and expression level of enzymes vary in different tissues and in pathological tissues. Therefore, enzyme has attracted significant interest as a stimulus to control the structure thus the function of peptides and proteins.

6.1. Design Principles

To design enzyme stimuli-responsive systems, enzyme responsive peptide linkers are often incorporated. A wide variety of such peptide linkers have been discovered to respond to various enzymes (Table 1). For example, matrix metalloproteinases (MMPs) play critical roles in tissue remodeling. An overexpression of MMP is associated with diseases such as cancer, cardiovascular diseases, arthritis, etc.[172] Cathepsin B is a member of endo/lysosomal proteases that involves in intracellular proteolysis, and is upregulated in cancer cells. MMP enzyme sensitive systems can be designed with linkers such as PLG/LAG, GPLG/V, PLG/VRG, GPLG/IAGQ where/indicates the cleavage site, and X in the G/X should have a small hydrophobic side chain (i.e., A, V, L, or I).[44] Cathepsin B enzyme sensitive systems often incorporate the peptide linker of GLFG.

The design of enzyme responsive systems normally adopts a modular approach, that is, they contain several segments and each segment exhibits one particular type of function. Based on the design principles, enzyme-responsive systems can be grouped into different categories, including 1) peptide-linker-drug conjugates and 2) polymer-linker-drug conjugates. These systems can either form nanoparticles or form the coating on NPs which are able respond to enzymes within the local microenvironment.

Several factors need to be considered when designing enzyme responsive segment. First, the segment should not only exhibit excellent enzyme specificity but also be compatible with the nanoparticle system. Second, the responsive segment should be accessible to the enzyme stimuli through the control of modular organization of the segment to increase or minimize enzyme access thus influencing
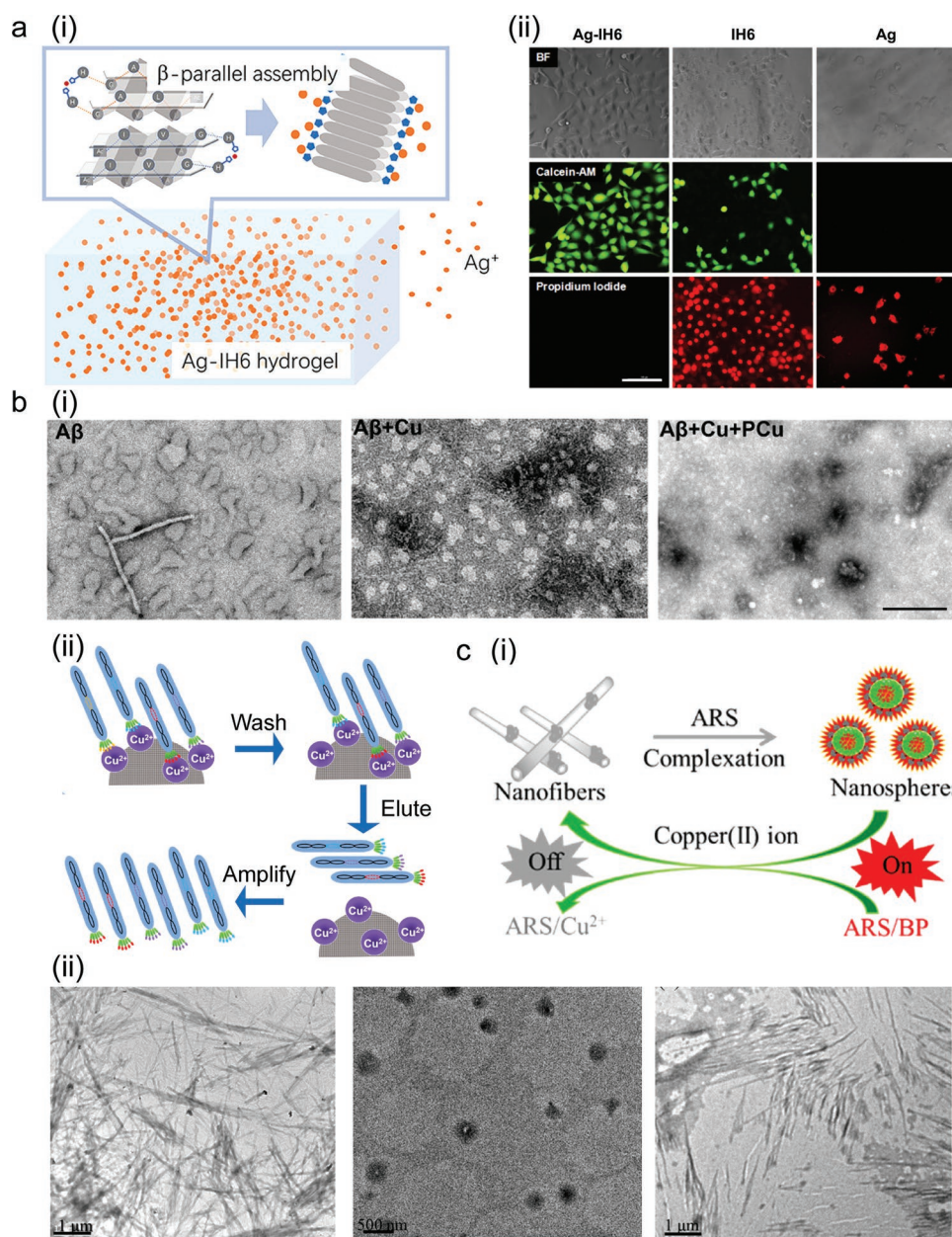
**ADVANCED
SCIENCE NEWS**

www.advancedsciencenews.com

**ADVANCED
FUNCTIONAL
MATERIALS**

www.afm-journal.de

Figure 12. a) (i) Schematic diagram of change in the structure of IH6 from antiparallel to parallel β-sheet upon silver ions addition. (ii) Fluorescence microscopy images of antibacterial behavior treated by Ag-IH6, IH6, and AgNO$_3$ in Hacat cells for 24 h (bar represents 100 µm). Reproduced with permission.[38] Copyright 2018, American Chemical Society. b) (i) TEM images aggregation of Aβ (left), Aβ and copper (middle), Aβ, copper and PCu (right). (ii) Illustration of phage display to derive copper-binding peptide sequences. Reproduced under the terms of CC-BY license.[171] Copyright 2021, the Authors, published by MDPI. c) (i) Schematic diagram of ARS/BP nanoindicator constructed and F fluorescence quenched upon copper addition. (ii) TEM images of BP peptides self-assemble into nanofibers (left). ARS/BP nanoindicator "turned on" (middle) and "turned off" by adding copper (right). Reproduced with permission.[40] Copyright 2021, American Chemical Society.

the enzyme reaction or response kinetics. Thirdly, the morphology change of the particle pre- and postcleavage should be purposely designed, either disintegrating into small molecules to enhance penetration or assembling into nanofires to improve retention that causes cytotoxic effects. In turn, the anticancer efficacy of the formed nanofibers correlates with the kinetics of nanofiber formation.[172] Therefore, based on these rational design rules, the response behavior of the enzyme-responsive systems can be optimized for

selective and tunable drug release thus achieving therapeutic functionalities.

To take the MMP enzyme responsive peptide linker PX$_1$G/LX$_2$G as an example, it can be designed to achieve controlled enzyme recognition and response kinetics, where/represents the cleavage site, and X$_1$ and X$_2$ positions can be any amino acids.[172] The 12 peptides represent a modular design with three segments (**Figure 13**a): 1) hydrophobic segment diphenylalanine (FF) on the N termini to drive the self-assembly of the
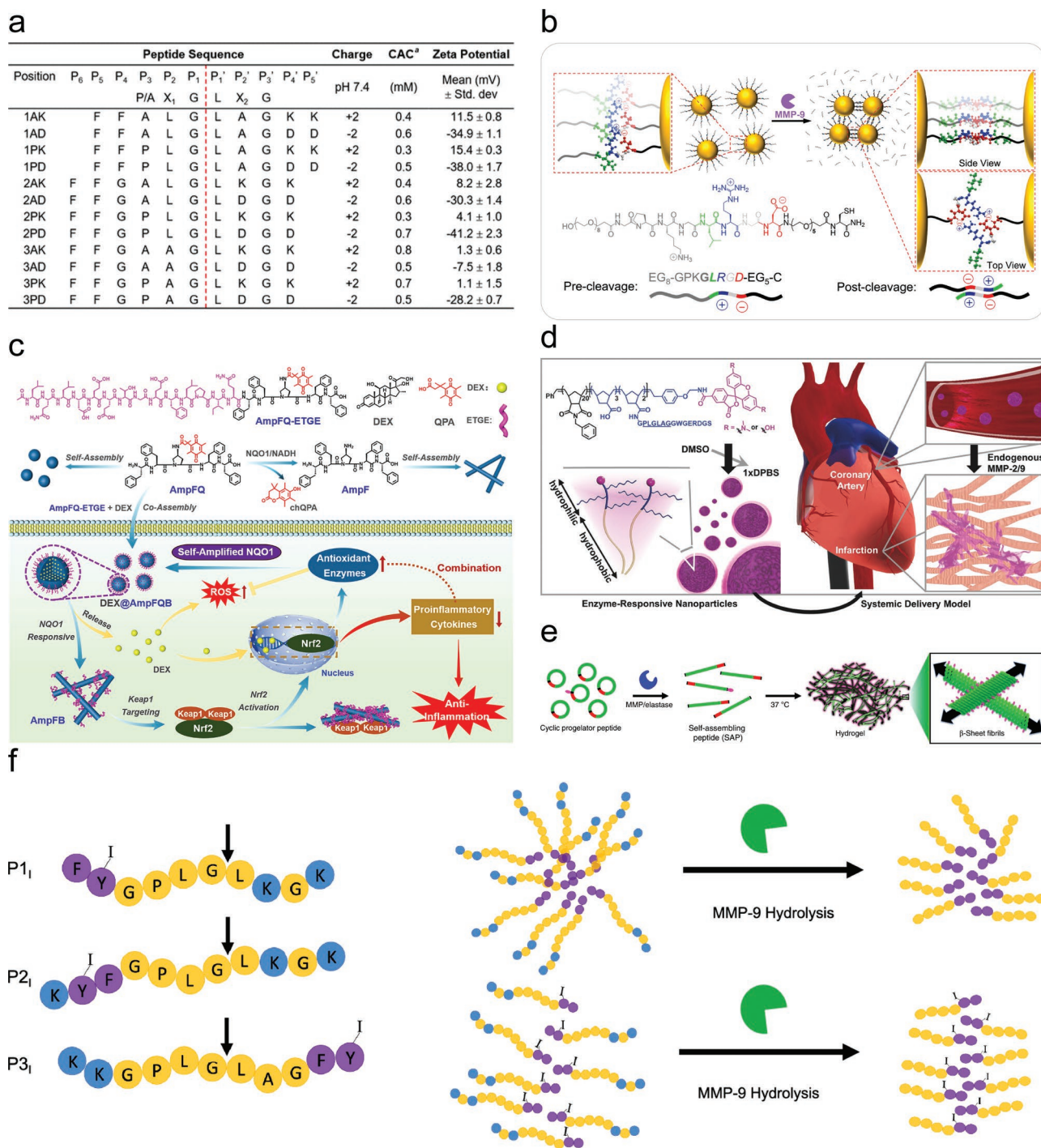
Figure 13. Enzyme responsive biomolecules. a) Different designed peptides that are responsive to MMP-9. Reproduced with permission.[172] Copyright 2019, American Chemical Society. b) Schematic illustration of MMP-9-triggered assembly of Au NPs using charge-complementary peptides. Reproduced with permission.[44] Copyright 2021, Wiley-VCH. c) Schematic illustration of the self-amplifying assembly of peptides in macrophages associated with the expression of NQO1. Reproduced with permission.[49] Copyright 2022, American Chemical Society. d) Diagram of a dye-labeled brush peptide–polymer amphiphile containing an MMP-2 and MMP-9 specific recognition sequence, shown underlined. Reproduced with permission.[53] Copyright 2015, Wiley-VCH. e) Design of cyclic, enzyme-responsive progelator peptides for activatable gelation. Reproduced with permission.[173] Copyright 2019, Springer Nature. f) Representations of P1I, P2I, and P3I indicating the functionally designed regions and sites of MMP-cleavage (arrows) and iodination (bracketed "I"). Reproduced with permission.[174] Copyright 2022, American Chemical Society.

postcleavage peptide as well as to bind hydrophobic drugs, 2) the MMP responsive segment (PX_1G/LX_2G) to control enzyme kinetics, and 3) hydrophilic segments with charges to modulate the electrostatic interaction between the peptide and the enzyme. By simply replacing a cationic amino acid (K) with an anionic amino acid (D), 2PK exhibits a conversion rate of

12-fold higher than that of the 2PD peptide demonstrating that the cationic peptides are cleaved preferentially by the anionic MMP enzyme. Furthermore, the enzymatic hydrolysis rate can be tuned by incorporating a particular amino acid. Among the cationic peptides, 1–3PK can be completely digested much quicker than 1–3AK with 1PK in 48 h as a result of the replacement of A with the Pro amino acid, as Pro is able to disrupt the assembly of secondary structures such as α-helices and β-sheets.

6.1.1. MMP Responsive Systems

MMPs are one of the most studied enzymes for enzyme-responsive systems as they are associated with various types of diseases, which can be exploited as an effective strategy for targeted delivery and controlled drug release. Zhang et al. integrated MMP-responsive peptide and zwitterionic EK polypeptides as a tumor-responsive and "sheddable" coating for spherical nucleic acids (EKEKEKEKEKEKEKEKEKEKE-KEEG-PLGLAG-dsDNA).[175] The EK polypeptides act as an antifouling shell or "cloaking ligand" to prolong the circulation time, while the peptide linker GPLGLAG is responsive to MMP enzyme. In the presence of MMPs, the EK polypeptide coating is cleaved, resulting in an increased cellular uptake of the spherical nucleic acids thus improved tumor accumulation. This is an ideal system that circulates longer in the presence of the shielding coating while becomes activated for enhanced cellular entry upon the enzyme stimuli-responsive cleavage of the coating in response to the MMP stimuli in targeted tumor tissues.

Alternatively, drugs can be integrated with MMP-responsive peptides. By purposely designing the peptide with a hydrophilic head and hydrophobic tail, the drug–peptide conjugate is able to self-assemble into nanoparticles for enzyme responsive drug release. Jia et al. designed a triblock molecule BBR-PLG-VRKLVFF-Ce6 (BPC) consisting of a hydrophilic chemotherapeutic drug berberrubine (BBR), an MMP-2 responsive peptide (PLGVRKLVFF), and a hydrophobic photosensitizer chlorin e6 (Ce6).[41] The PLGVR could be specifically cleaved by MMP-2, while KLVFF derived from the amyloid beta (Aβ) peptide is able to form β-sheet thus nanofibers. In the presence of MMP-2 in tumor microenvironment, the self-assembled nanoparticles are cleaved at the MMP-2 responsive site, leading to the release of chemotherapeutic drug BBR to kill tumor cells as well as the formation of nanofibers with Ce6, which can be retained at the tumor site for a much longer time. Jiang et al. developed a multifunctional peptide (P51) for targeted delivery of a hydrophobic chemodrug pirarubicin (THP).[176] P51 consists of a specific targeting ligand (RGD) and three tumor microenvironment responsive triggers that can be triggered by a reducing agent, MMP-2 enzyme, and acid environment. It contains an α-helix 41-residue peptide and a negatively charged peptide sequence (SEEDP), which is capable of encapsulating pirarubicin via hydrophobic and electrostatic interactions, a Cys-s-s-Cys disulfide linker for cleavage in response to the reducing environment (DTT) in tumor, and an MMP-2 responsive peptide linker (PVGLIG). Therefore, the P51 and the hydrophobic drug pirarubicin self-assembled into spherical nanoparticles

(P51-THP NPs) in a single step and the P51-THP NPs demonstrated controlled drug release responsive to three triggers including acid condition, DTT and MMP-2. In the presence of these three triggers, the release efficiency was significantly enhanced leading to more effective tumor targeting and antitumor effect. Cao et al. reported a smart drug carrier for targeted cancer drug delivery based on a surfactant like peptide (Nap-FFGPLGLARKRK).[42] This peptide comprises three functional modules: the aromatic Nap-FF for fibril formation, the MMP-7 responsive motif GPLGLA, and the positively charged RKRK motif to adjust amphiphilicity and to facilitate specific interaction with cell membrane. The surfactant like peptide is able to self-assemble into long fibrils with hydrophobic cores, which allow the encapsulation of a large amount of hydrophobic anticancer drug doxorubicin. When the assembled long fibrils arrive at the tumor site, they are cleaved by MMP-7 into smaller ones resulting in improved antitumor efficiency and reduced site effects.

Therapeutic protein–polypeptide conjugates, similar to protein–polymer conjugates, have been developed to enhance drug pharmacokinetic properties. Wang et al. designed a therapeutic protein interferon (IFN) polypeptide (poly(γ-(2-(2-(2-methoxyethoxy)ethoxy)ethyl-L-glutamate) P(EG$_3$Glu)$_{20}$) conjugate consisting of an MMP-responsive peptide segment (GPLGVRGK).[177] After cleavage by the MMP-2 at the tumor site, the protein IFN-polypeptide converts to IFN thus shrinking significantly in size which is helpful for tumor penetration due to its smaller size. Compared to the nonresponsive analogue protein–polypeptide conjugate, the MMP-responsive one showed superior tumor retention, deeper tumor penetration, and excellent antitumor efficacy using both OVCAR3 and SKOV3 ovarian cancer mice models, demonstrating protein-polypeptide is a valid approach to improve cancer drug delivery. Guo et al. designed an MMP-responsive polymer MePEG-peptide-PETPCL incorporating an MMP cleavable peptide (GPLGIAGQ) and a penetrating peptide (R9) for enhanced selective drug release as well as improved cell penetration toward targeted cancer therapy.[43]

Nanoparticles can be coated with enzyme responsive peptides to direct cell fate. Gold nanoparticles were modified with zwitterionic peptides containing an MMP-responsive site (EG$_8$-GPKG/LRGD-EG$_5$-C-Au NPs), which are positively charged at physiological pH to attract the negatively charged MMP ensuring enhanced interaction (Figure 13b).[44] The cystine at the terminal facilitates the thiol–gold binding, and the RGD sequence plays two roles. One is to induce the aggregation of Au NPs via electrostatic interaction upon peptide cleavage and another is to bind to cancer cells that present overexpressed $\alpha\nu\beta3$ integrin receptors. When these modified Au NPs were incubated with triple negative breast cancer cells which have higher expressions of MMP-9 and integrin on the cell surface, a significantly decreased cell viability was observed. The presence of MMP-9 cleaves the zwitterionic peptide leading to the formation of Au NP aggregates via RGD driven electrostatic interaction. Consequently, these Au NP aggregates are internalized via an actin dependent micropinocytosis thus enhanced cytotoxicity.

Similarly, gold nanorods were fabricated with Tat-MMP responsive segment and a zwitterionic peptide coating (CCVVGRKKRRQRRRPQG-GPLGV-EKEKEKEK) for enhanced

**ADVANCED
SCIENCE NEWS**

www.advancedsciencenews.com

**ADVANCED
FUNCTIONAL
MATERIALS**

www.afm-journal.de

photothermal therapy.[45] The coating consists of a cationic Tat peptide (GRKKRRQRRRPQ) derived from the HIV-1 Tat protein for cell penetration, an MMP-9 responsive segment (GPLGV) for MMP enzyme responsive cleavage and a zwitterionic antifouling sequence with alternative E and K (EKEKEKEK) for long circulation. Therefore, the peptide-modified gold nanorods showed long circulation as well as enhanced cellular uptake thus efficient photothermal therapy.

6.1.2. Cathepsin B Responsive Systems

Cathepsin B as a lysosomal protease plays critical roles in intracellular proteolysis. Many invasive and metastatic cancers overexpress cathepsin B. Unlike MMP enzymes that are upregulated in extracellular microenvironments, cathepsin B is richer intracellularly. Various cathepsin B responsive systems have been designed by incorporating the peptide linker GFLG, and the postcleavage peptides normally target at a subcellular organelle such as mitochondria.

Peptides and drugs can be covalently linked to form a prodrug. Zhang et al. developed a PEGylated dendrimer-GFLG-gemcitabine system using the highly efficient click chemistry.[46] The antitumor drug gemcitabine was conjugated to the C-terminus of GFLG peptide, with the N-terminus of the peptide conjugated to a PEGylated dendrimer NP. The obtained NP is sensitive to cathepsin B therefore showing a significantly faster drug release. Alternatively, hydrophobic amino acids or other functional molecules can be incorporated into the peptide to facilitate drug encapsulation via hydrophobic interaction. Song and Choi designed amphiphilic peptides containing the cathepsin B-sensitive peptide GFLG and charged amino acids RH to encapsulate the hydrophobic drug doxorubicin.[178] Three peptides were designed including RH-(GFLG)$_1$, RH-(GFLG)$_2$, and RH-(GFLG)$_3$. Because of the strong hydrophobicity of F and L amino acids and the positive charge of R, the peptide RH-(GFLG)$_3$ can self-assemble into NPs with doxorubicin residing in the hydrophobic core, whereas RH-(GFLG)$_1$ and RH-(GFLG)$_2$ cannot self-assemble due to the lack of hydrophobicity. In addition, the positively charged R functions as a cell-penetrating peptide that increases cellular uptake, and the H containing the imidazole ring endows the NP endo/lysosomal escape capability owing to its proton buffering capacity. Similarly, a dual-targeting peptide amphiphile–photosensitizer conjugate pPAC (PpIX-GGGK(TPP)GG-GFLG-R$_7$-RGD) was designed to encapsulate doxorubicin.[179] The amphiphilic pPAC forms core–shell nanomicelles with DOX trapped in the core. The RGD as a tumor-targeting ligand promotes endocytosis, and the R$_8$ segment improves cell penetrating. Upon endocytosis, the GFLG linker can be cleaved by cathepsin B, leading to the rapid release of DOX and PpIX-peptide. At the same time, the accumulated photosensitizer PpIX in the subcellular mitochondria generates reactive oxygen species (ROS) under light irradiation, thus achieving the synergistic chemotherapy and photodynamic therapy.

Gold nanoparticles have been combined with cathepsin B-sensitive peptides for enhanced photothermal- or radiotherapy. Ding et al. designed an Au NP-Tat-GFLG-(EK)$_5$ system to target nucleus.[180] Au NPs were immobilized via a CCV linker with

a nucleus targeting peptide Tat (GRKKRRQRRRPQ). A cathepsin B-sensitive linker V-GFLG-V was conjugated to Tat, and an antifouling peptide (EK)$_5$ (EKEKEKEKEK) was further conjugated to Tat, enabling long circulation thus passive tumor accumulation. After cleaved by cathepsin B, Au NP-Tat can target nucleus and demonstrate superior radio-sensitizing cytotoxicity with X-ray irradiation. Similarly, Jin et al. developed an Au nanorod-CC-EKEK-V-F*d*-RFKF*d*-RFK-V-GFLG-V-EKEKEKEKEKEK system for mitochondria-targeted photothermal therapy.[181]

6.1.3. Others

Other than MMP families and cathepsin B, many other enzymes have also been explored to trigger the conformational change of peptides and proteins. Gong et al. developed a nanoparticle-to-nanofiber switching system based on an alkaline phosphatase (ALPase)-sensitive peptide Ac-AAAAAA-pY-RGD-NH$_2$.[47] The amphiphilic peptide can self-assemble into NPs and encapsulate hydrophobic doxorubicin in the core, exposing the tumor targeting ligand RGD on the NP surface. The phosphorylated tyrosine (pY) can be cleaved by the abnormally high expression of ALPase in tumor sites, leading to the switch of nanoparticles to nanofibers thus intracellular drug release, and the formation of A6 nanofibers improves drug retention.

Main protease (Mpro), also known as 3CLpro, is a nonstructural protein capable of effectively cleaving the viral precursor polyprotein at specific sites to produce functional proteins. Mpro is a promising target for virus detection and inhibition. Cheng et al. designed a sophisticated peptide (PyTPE-KLVFF-GGG-SAVLQ/SGFRKMA-RRRRRR) responding to main protease (Mpro).[48] The R$_6$ increases the solubility of the peptide and improves cell-penetration. SAVLQ/SGFRKMA (/ indicates the cleavage site) can be cleaved by Mpro which is overexpressed by SARS-CoV-2-infected cells. GGG is a linker to provide more flexibility and reduce steric hindrance. After the cleavage of the hydrophilic part SGFRKMA-RRRRRR, KLVFF derived from a β-amyloid (Aβ) protein can form insoluble fibrils thus killing the SARS-CoV-2 infected cells.

Quinone dehydrogenase 1 (NQO1) is a cytosolic quinone reductase that plays an important role in suppressing oxidative stress. NQO1 is often upregulated in various types of tumor cells, thus allowing for the development of NQO1-responsive systems. Song et al. designed a dexamethasone-loaded self-amplifying system using the peptide LQLDEETGEFLPIQ-FF-Amp(QPA)-FF for treating acute lung injury (Figure 13c).[49] Quinone propionic acid (QPA) is a moiety sensitive to the enzyme NQO1, and can be cleaved off, leaving the postcleavage peptide LQLDEETGEFLPIQ-FF-Amp-FF assembling into nanofibrils. LQLDEETGEFLPIQ is a targeting ligand to Kelch ECH-associated protein 1 which can upregulate the expression of NQO1, consequently further promoting the degradation of LQLDEETGEFLPIQ-FF-Amp(QPA)-FF. In this way, a self-amplifying relationship between peptide assembly and NQO1 expression was established for passive targeted delivery of dexamethasone to acute injured lungs.

Furin enzyme is an important endoprotease overexpressed in many types of cancers. Cheng et al. reported a pH- and

furin- responsive peptide coated gold NP system for sensitive imaging and efficient therapy of tumors.[50] Au NPs were conjugated with polyethylene glycol derivate SH-PEG-COOH and peptide RRVR, which can be cleaved by furin. After cleavage at an acidic pH, the surface charge of Au NPs was switched to be zwitterionic, thus promoting electrostatic aggregation, resulting in enhanced photoacoustic imaging and photothermal effects.

Enzyme-responsive peptides have also been used in bulk materials such as hydrogel. Zhou et al. developed a hydrogel using the peptide 4-formylbenzamide-V/KV/KV/K (/ indicates cleavage site) that can be triggered. A gel-to-sol transition occurs upon the addition of human neutrophil elastase secreted by neutrophils responding to inflammation.[51] The hydrogel exhibited more and longer H_2S release compared to untriggered gels, which is helpful in reducing inflammation.

6.2. Applications

Among the various stimuli, enzyme-responsive systems have garnered significant attention due to the mild reaction conditions and low side effects.[182] In light of the overexpression of different enzymes at the local environment of targeted tissues, enzyme-responsive systems have been designed for targeted drug-delivery and diagnostics, or the combination of diagnostics and treatment—theranostics.[174] The strategy is to incorporate an enzyme responsive peptide segment in peptide, proteins, polymers or drugs to either forming nanocarriers or coating nanoparticles for targeted drug delivery.[175,183] A large variety of enzyme responsive peptide/protein systems have been developed for targeted cancer delivery to achieve programmed drug release, enhanced penetration, better tumor attention as well as improved tumor targeting, as many enzymes are overexpressed in the tumor microenvirnment (MMP, cathepsin B, etc.). Many different examples have been discussed in Section 6.1 for cancer targeted delivery, this section mainly focuses on applications in other diseases highlighting the great potentials of enzyme-responsive systems for a wide range of diseases.

MMP-2 has been discovered to be overexpressed in renal tissue during acute kidney injury (AKI). A sialic acid–dextran–PVGLIG–curcumin (SA–DEX–PVGLIG–CUR) polymeric prodrug system was designed with an MMP-2 responsive peptide segment for targeted AKI therapy.[52] Sialic acid is incorporated as the ligand targeting to the E-selection receptors on the inflamed vascular endothelial cells, and the PVGLIG is MMP-2 responsive allowing rapid release of the anti-inflammatory drug curcumin at the targeted injury site. This prodrug increases the water solubility of curcumin significantly. When it was mixed with a medium containing MMP-2, the release rate of CUR was significantly enhanced compared to the SA–DEX–CUR which does not respond to MMP-2. In vivo mice experiments demonstrated rapid and enhanced renal accumulation of SA–DEX–PVGLIG–CUR in AKI mice, and the rapid drug release inhibited the pathological progression of AKI effectively compared to both the free drug and nonenzyme responsive prodrugs, demonstrating the great potential of enzyme-responsive systems for AKI treatment.[52]

MMP enzyme-responsive nanoparticles have also been developed for targeted acute myocardial infarction (MI)

delivery.[53] The nanoparticle is made of a peptide polymer amphiphile consisting of a polynorbornene backbone and a peptide sequence (GPLGLAGGWERDGS) specific to enzymes (MMP-2 and MMP-9), which present at the acute MI. After IV injection, the nanoparticles circulate freely in the bloodstream, and then reach the infarct through the leaky post-MI vasculature where they undergo a morphological change from discrete micelle particles into network-like scaffolds in responding to the enzymatic stimuli MMP-2 and MMP-9, leading to their long retention at the injured site for up to 28 days postinjection (Figure 13d). By controlling the hydrophilic weight fraction, the enzyme responsiveness can be tuned. For example, when it was decreased from 0.55 to 0.45 by decreasing the peptide density, the responsiveness of the nanoparticles increased significantly.[53] On the other hand, injectable biopolymer hydrogels have attracted great interests to boost cardiac function and prevent harmful left ventricular remodeling post-MI. However, most hydrogels reported for preclinical studies are not suitable for minimally invasive catheter delivery because of their excess viscosity, rapid gelation, and/or concerns about hemocompatibility as well as potential for embolism. Carlini et al. developed enzyme-responsive progelator cyclic peptides for minimally invasive MI delivery (Figure 13e).[173] They designed sterically constrained cyclic peptides which can flow freely for easy injection, followed by rapidly assembling into hydrogels upon linearization by MMP and elastase enzymes. This material can flow through a syringe or a cardiac injection catheter without gelation or clogging, while becomes a gel at the MI site in rat models demonstrating the great potential for MI delivery. These enzyme-responsive systems provide a promising approach for targeted delivery at acute MI.

MMP-responsive spherical micelles have been fabricated for cancer immunotherapeutic delivery. Basically, amphiphilic diblock copolymers based on norbornene monomers were designed with one block containing hydrophobic Toll-like receptor 7 (TLR7) agonists, and the other block containing hydrophilic peptides responsive to MMPs.[184] Upon dialysis against buffer solution, the copolymers form spherical micelles of 15 nm in size. Subsequent exposure to MMP-9 enzymes induces a morphological transition from spherical micelles to microscale assemblies resulting in their prolonged retention at the tumor site. The IV administration of the micelles to 4T1 breast cancer mice showed excellent nanoparticle tumor accumulation and retention, significant primary tumor growth suppression, lung metastases inhibition as well as decreased immunotoxicity. The enzyme-responsive system provides a potential platform for cancer immunotherapy.[184]

Antibiotic resistance presents a big challenge for treating common infections. The development of an infection-responsive delivery system offers a possible strategy to mitigate multidrug resistance. Recent studies have showed an increase in thrombin-like activity during *Staphylococcus aureus* infection, so smart drug release responsive to infection becomes attractive. Thrombin, a human protease, cleaves fibrinogen at the R–G bonds with a unique specificity. A nanoparticle delivery vehicle was designed using a recombinant spider silk protein with a thrombin-sensitive linker embedded. The spider silk protein as a drug carrier allows the encapsulation of a large amount of the drug with good stability. Local enzyme-responsive release of

antibiotic drugs ensures the targeted release of the drug at the disease site.[54]

In addition to their therapeutic applications, enzyme triggered systems have also been applied in imaging or diagnostics. The incorporation of MMP-responsive peptide with a radioactive isotope of iodine provides an approach to probe the MMP-9 activity at MMP-expressing tumors (Figure 13f).[174] Among the MMP-9 responsive peptides containing tyrosine or iodotyrosine, the one containing iodotyrosine showed more rapid response and more complete cleavage by MMP-9. Upon cleavage by MMP, the residual peptide self-assembles into fibers resulting in their accumulation at the MMP-9 secreting sites thus enhanced radioactive signal for better imaging.

7. Conclusions and Outlook

In summary, this review paper offers an overview of recent innovations in designing stimuli-responsive biomolecules with an emphasis on conformational shifts and property changes. Various critical physiochemical triggers including temperature, pH, light, ions, and enzyme have been investigated and concisely summarized to give an in-depth exploration of designing purposes, underlying responding mechanisms and their applications. In addition, we take a close look at the amino acid sequences and link the sequences with the structural shift to offer a better understanding of the stimuli-responsive behaviors. The designed peptides and proteins presented in this review illustrate the development in this field over the past 20 years and offer a glimpse of exciting future opportunities. The understanding of the embedded concepts and mechanisms would facilitate and inspire future researchers to explore novel designs for various exciting applications.

Tremendous progress has been made in developing stimuli-responsive peptides and proteins. Predictions over the conformational structure can be made by having a closer look at the biomolecule sequences and the interactions between the amino residues which allows us to design a target-functional peptide or protein. For example, the transition temperature for ELP-fusion proteins can be precisely predicted and controlled by adjusting the number of repeats of VPGXG, the hydrophobicity of the guest residues, and the linker sequences. Moreover, new efforts have been directed to develop dual-responsive biomolecules by combining temperature with pH[185] or temperature with light[186] in many applications such as biocatalysis,[187] drug delivery,[188] coatings,[189] sensors, and microengines.[190]

Nevertheless, key challenges remain as follows.

1) One of the main limitations observed is the understanding of the underlying mechanisms. While the general structure changes can be monitored through a wide range of tools such as scanning electron and atomic force microscopy. The fundamental understanding of interactions at the molecular level is lacking, which warrants future efforts.
2) Prediction over the structural shifts of designed biomolecules is challenging due to the complexity of protein structures and dynamic environmental changes. Although simulation can help to mimic how the proteins and peptides behave in different conditions. The accurate prediction in a time-efficient manner remains challenging.
3) Another issue is the precise control over the transition point. In most cases, the structural shift and thus property variations occur in a narrow range of conditions. Accurate control over the transition requires a full understanding of the transition point and surrounding conditions. A typical example is that targeted drug delivery requires a drug to be released only at the specific sites to act on abnormal cells. In other words, the nanocarriers designed have to remain stable but release at the local environment of specific sites.

In conclusion, it is clear that stimuli-responsive biomolecules have brought great benefits to many bioinspiration approaches. However, exploration will continue to engage the existing challenges. Last but not the least, we appreciate all the efforts researchers have put into this field to enable us to summarize and present their impressive work in this review.

Conflict of Interest

The authors declare no conflict of interest.

[1] a) A. Chilkoti, M. R. Dreher, D. E. Meyer, *Adv. Drug Delivery Rev.* **2002**, *54*, 1093; b) D. Chow, M. L. Nunalee, D. W. Lim, A. J. Simnick, A. Chilkoti, *Mater. Sci. Eng., R* **2008**, *62*, 125; c) M. Haider, Z. Megeed, H. Ghandehari, *J. Controlled Release* **2004**, *95*, 1; d) E. R. Welsh, D. A. Tirrell, *Biomacromolecules* **2000**, *1*, 23.

[2] R. J. Wilson, Y. Li, G. Yang, C.-X. Zhao, *Particuology* **2022**, *64*, 85.

[3] D. W. P. M. Lowik, E. H. P. Leunissen, M. van den Heuvel, M. B. Hansen, J. C. M. van Hest, *Chem. Soc. Rev.* **2010**, *39*, 3394.

[4] a) R. Fang, J. Pi, T. Wei, A. Ali, L. Guo, *Polymers* **2021**, *13*, 2089; b) F. Ercole, T. P. Davis, R. A. Evans, *Polym. Chem.* **2010**, *1*, 37; c) L. A. Wells, F. Lasowski, S. D. Fitzpatrick, H. Sheardown, *Crit. Rev. Biomed. Eng.* **2010**, *38*, 487; d) S. Dai, P. Ravi, K. C. Tam, *Soft Matter* **2009**, *5*, 2513.

[5] a) S. Litvinchuk, H. Tanaka, T. Miyatake, D. Pasini, T. Tanaka, G. Bollot, J. Mareda, S. Matile, *Nat. Mater.* **2007**, *6*, 576;

b) S. Litvinchuk, G. Bollot, J. Mareda, A. Som, D. Ronan, M. R. Shah, P. Perrottet, N. Sakai, S. Matile, *J. Am. Chem. Soc.* **2004**, *126*, 10067; c) Y. Liu, G. Yang, Y. Hui, S. Ranaweera, C. X. Zhao, *Small* **2022**, *18*, 2106580; d) J. J. Cornelissen, J. J. Donners, R. de Gelder, W. S. Graswinckel, G. A. Metselaar, A. E. Rowan, N. A. Sommerdijk, R. J. Nolte, *Science* **2001**, *293*, 676.

[6] M. Egli, S. Zhang, *Nat. Rev. Mol. Cell Biol.* **2022**, *23*, 165.

[7] H. Dong, J. D. Hartgerink, *Biomacromolecules* **2007**, *8*, 617.

[8] S. G. Zhang, A. Rich, *Proc. Natl. Acad. Sci. USA* **1997**, *94*, 23.

[9] M. De Zotti, V. N. Syryamina, R. Hussain, E. Longo, G. Siligardi, S. A. Dzuba, L. Stella, F. Formaggio, *ChemBioChem* **2019**, *20*, 2125.

[10] D. Zhu, H. Wang, P. Trinh, S. C. Heilshorn, F. Yang, *Biomaterials* **2017**, *127*, 132.

[11] S. R. MacEwan, A. Chilkoti, *Nano Lett.* **2014**, *14*, 2058.

[12] a) K. M. Luginbuhl, J. L. Schaal, B. Umstead, E. M. Mastria, X. H. Li, S. Banskota, S. Arnold, M. Feinglos, D. D'Alessio, A. Chilkoti, *Nat. Biomed. Eng.* **2017**, *144*; b) M. Amiram, K. M. Luginbuhl, X. Li, M. N. Feinglos, A. Chilkoti, *J. Controlled Release* **2013**, *172*, 144.

[13] S. Roberts, V. Miao, S. Costa, J. Simon, G. Kelly, T. Shah, S. Zauscher, A. Chilkoti, *Nat. Commun.* **2020**, *1*, 1342.

[14] D. Mozhdehi, K. M. Luginbuhl, J. R. Simon, M. Dzuricky, R. Berger, H. S. Varol, F. C. Huang, K. L. Buehne, N. R. Mayne, I. Weitzhandler, M. Bonn, S. H. Parekh, A. Chilkoti, *Nat. Chem.* **2018**, *10*, 496.

[15] C. Minelli, J. X. Liew, M. Muthu, H. Andresen, *Soft Matter* **2013**, *9*, 5119.

[16] B. Apostolovic, H.-A. Klok, *Biomacromolecules* **2008**, *9*, 3173.

[17] a) A. F. Dexter, A. S. Malcolm, A. P. J. Middelberg, *Nat. Mater.* **2006**, *5*, 502; b) S. S. J. Leong, A. P. J. Middelberg, *Protein Sci.* **2006**, *15*, 2040; c) A. S. Malcolm, A. F. Dexter, A. P. J. Middelberg, *Soft Matter* **2006**, *2*, 1057.

[18] Y. Hui, D. Wibowo, C. X. Zhao, *Langmuir* **2016**, *32*, 822.

[19] A. P. J. Middelberg, M. Dimitrijev-Dwyer, *ChemPhysChem* **2011**, *12*, 1426.

[20] A. Aggeli, M. Bell, L. M. Carrick, C. W. G. Fishwick, R. Harding, P. J. Mawer, S. E. Radford, A. E. Strong, N. Boden, *J. Am. Chem. Soc.* **2003**, *125*, 9619.

[21] M. Altman, P. Lee, A. Rich, S. Zhang, *Protein Sci.* **2000**, *9*, 1095.

[22] B. Frohm, J. E. DeNizio, D. S. Lee, L. Gentile, U. Olsson, J. Malm, K. S. Akerfeldt, S. Linse, *Soft Matter* **2015**, *11*, 414.

[23] U. Shimanovich, A. Levin, D. Eliaz, T. Michaels, Z. Toprakcioglu, B. Frohm, E. De Genst, S. Linsey, K. S. Akerfeldt, T. P. J. Knowles, *Small* **2021**, *17*, 2007188.

[24] a) A. Sánchez-Ferrer, J. Adamcik, S. Handschin, S. H. Hiew, A. Miserez, R. Mezzenga, *ACS Nano* **2018**, *12*, 9152; b) S. H. Hiew, P. A. Guerette, O. J. Zvarec, M. Phillips, F. Zhou, H. Su, K. Pervushin, B. P. Orner, A. Miserez, *Acta Biomater.* **2016**, *46*, 41; c) S. H. Hiew, A. Sánchez-Ferrer, S. Amini, F. Zhou, J. Adamcik, P. Guerette, H. Su, R. Mezzenga, A. Miserez, *Biomacromolecules* **2017**, *18*, 4240.

[25] J. G. Ray, S. S. Naik, E. A. Hoff, A. J. Johnson, J. T. Ly, C. P. Easterling, D. L. Patton, D. A. Savin, *Macromol. Rapid Commun.* **2012**, *33*, 819.

[26] B.-X. Zhao, Y. Zhao, Y. Huang, L.-M. Luo, P. Song, X. Wang, S. Chen, K.-F. Yu, X. Zhang, Q. Zhang, *Biomaterials* **2012**, *33*, 2508.

[27] T. J. Moyer, J. A. Finbloom, F. Chen, D. J. Toft, V. L. Cryns, S. I. Stupp, *J. Am. Chem. Soc.* **2014**, *136*, 14746.

[28] J. P. Schneider, D. J. Pochan, B. Ozbas, K. Rajagopal, L. Pakstis, J. Kretsinger, *J. Am. Chem. Soc.* **2002**, *124*, 15030.

[29] G. Zhang, L. Zhang, H. Rao, Y. Wang, Q. Li, W. Qi, X. Yang, R. Su, Z. He, *J. Colloid Interface Sci.* **2020**, *577*, 388.

[30] F. Novelli, A. Strofaldi, S. De Santis, A. Del Giudice, S. Casciardi, L. Galantini, S. Morosetti, N. V. Pavel, G. Masci, A. Scipioni, *Langmuir* **2020**, *36*, 3941.

[31] A. S. Carlini, W. Choi, N. C. McCallum, N. C. Giannneschi, *Adv. Funct. Mater.* **2021**, *31*, 2007733.

[32] J. Sun, C. Ma, S. Maity, F. Wang, Y. Zhou, G. Portale, R. Göstl, W. H. Roos, H. Zhang, K. Liu, A. Herrmann, *Angew. Chem., Int. Ed.* **2021**, *60*, 3222.

[33] B. Israeli, D. S. Strugach, S. Gelkop, S. Weber, D. S. Gozlan, M. Amiram, *Adv. Funct. Mater.* **2021**, *31*, 2011276.

[34] L. Yin, H. Tang, K. H. Kim, N. Zheng, Z. Song, N. P. Gabrielson, H. Lu, J. Cheng, *Angew. Chem., Int. Ed.* **2013**, *52*, 9182.

[35] a) B. Bulutoglu, S. J. Yang, S. Banta, *Biomacromolecules* **2017**, *18*, 2139; b) B. Bulutoglu, K. Dooley, G. Szilvay, M. Blenner, S. Banta, *ACS Synth. Biol.* **2017**, *6*, 1732.

[36] J. S. Yuan, Y. Zhang, Y. Sun, Z. C. Cai, L. J. Yang, H. Lu, *Biomacromolecules* **2018**, *19*, 2089.

[37] J. Borglin, R. Selegard, D. Aili, M. B. Ericson, *Nano Lett.* **2017**, *17*, 2102.

[38] Y. Guo, S. Wang, H. Du, X. Chen, H. Fei, *Biomacromolecules* **2019**, *20*, 558.

[39] A. D'Souza, J. H. Yoon, H. Beaman, P. Gosavi, Z. Lengyel-Zhand, A. Sternisha, G. Centola, L. R. Marshall, M. D. Wehrman, K. M. Schultz, M. B. Monroe, O. V. Makhlynets, *ACS Appl. Mater. Interfaces* **2020**, *12*, 17091.

[40] J.-Q. Feng, D.-K. Shi, W.-Q. Ding, Y.-J. Cheng, S.-Y. Qin, A.-Q. Zhang, *ACS Biomater. Sci. Eng.* **2021**, *7*, 3361.

[41] W. F. Jia, R. Liu, Y. S. Wang, C. A. Hu, W. Q. Yu, Y. Zhou, L. Wang, M. J. Zhang, H. L. Gao, X. Gao, *Acta Pharm. Sin. B* **2022**, *12*, 3354.

[42] M. W. Cao, S. Lu, N. N. Wang, H. Xu, H. Cox, R. H. Li, T. Waigh, Y. C. Han, Y. L. Wang, J. R. Lu, *ACS Appl. Mater. Interfaces* **2019**, *11*, 16357.

[43] F. Y. Guo, Q. F. Fu, C. H. Jin, X. G. Ji, Q. Y. Yan, Q. L. Yang, D. J. Wu, Y. Gao, W. Y. Hong, A. Q. Li, G. S. Yang, *Drug Delivery* **2019**, *26*, 1027.

[44] R. H. Huang, N. Nayeem, Y. He, J. Morales, D. Graham, R. Klajn, M. Contel, S. O'Brien, R. V. Ulijn, *Adv. Mater.* **2022**, *34*, 2104962.

[45] L. M. Wu, B. Y. Lin, H. Yang, J. Chen, Z. W. Mao, W. L. Wang, C. Y. Gao, *Acta Biomater.* **2019**, *86*, 363.

[46] C. Y. Zhang, D. Y. Pan, J. Li, J. N. Hu, A. Bains, N. Guys, H. Y. Zhu, X. H. Li, K. Luo, Q. Y. Gong, Z. W. Gu, *Acta Biomater.* **2017**, *55*, 153.

[47] Z. Y. Gong, B. L. Zhou, X. Y. Liu, J. J. Cao, Z. X. Hong, J. Y. Wang, X. R. Sun, X. M. Yuan, H. N. Tan, H. J. Ji, J. K. Bai, *ACS Appl. Mater. Interfaces* **2021**, *13*, 55913.

[48] Y. Cheng, A. E. Clark, J. J. Zhou, T. Y. He, Y. Li, R. M. Borum, M. N. Creyer, M. Xu, Z. C. Jin, J. C. Zhou, W. Yim, Z. H. Wu, P. Fajtova, A. J. O'Donoghue, A. F. Carlin, J. V. Jokerst, *ACS Nano* **2022**, *16*, 12305.

[49] Y. Q. Song, M. M. Li, N. Song, X. Liu, G. Y. Wu, H. Zhou, J. F. Long, L. Q. Shi, Z. L. Yu, *J. Am. Chem. Soc.* **2022**, *144*, 6907.

[50] X. J. Cheng, X. X. Zhou, J. W. Xu, R. Sun, H. W. Xia, J. A. Ding, Y. E. Chin, Z. F. Chai, H. B. Shi, M. Y. Gao, *Anal. Chem.* **2021**, *93*, 9277.

[51] M. J. Zhou, Y. Qian, Y. M. Zhu, J. Matson, *Chem. Commun.* **2020**, *56*, 1085.

[52] J. B. Hu, D. Liu, J. Qi, K. J. Lu, F. Y. Jin, X. Y. Ying, J. You, Y. Z. Du, *Biomater. Sci.* **2018**, *6*, 3397.

[53] M. M. Nguyen, A. S. Carlini, M. P. Chien, S. Sonnenberg, C. L. Luo, R. L. Braden, K. G. Osborn, Y. W. Li, N. C. Giannneschi, K. L. Christman, *Adv. Mater.* **2015**, *27*, 5547.

[54] P. Mulinti, J. Shreffler, R. Hasan, M. Dea, A. E. Brooks, *Pharmaceutics* **2021**, *13*, 1358.

[55] L. Szkolar, J.-B. Guilbaud, A. F. Miller, J. E. Gough, A. Saiani, *J. Pept. Sci.* **2014**, *20*, 578.

[56] A. Barve, A. Jain, H. Liu, W. Jin, K. Cheng, *Nanomedicine* **2016**, *12*, 2373.

[57] H. Komori, Y. Inai, *J. Org. Chem.* **2007**, *72*, 4012.

[58] a) M. R. Banki, L. A. Feng, D. W. Wood, *Nat. Methods* **2005**, *2*, 659; b) R. L. M. Teeuwen, F. A. de Wolf, H. Zuilhof, J. C. M. van Hest,

**ADVANCED
SCIENCE NEWS**
www.advancedsciencenews.com

**ADVANCED
FUNCTIONAL
MATERIALS**
www.afm-journal.de

Soft Matter **2009**, *5*, 4305; c) D. E. Meyer, K. Trabbic-Carlson, A. Chilkoti, *Biotechnol. Prog.* **2001**, *17*, 720; d) D. E. Meyer, G. A. Kong, M. W. Dewhirst, M. R. Zalutsky, A. Chilkoti, *Cancer Res.* **2001**, *61*, 1548.

[59] a) A. Bandiera, L. Corich, S. Tommasi, M. De Bortoli, P. Pelizzo, M. Stebel, D. Paladin, S. Passamonti, *Biotechnol. Bioeng.* **2020**, *117*, 354; b) M. S. Bahniuk, A. K. Alshememry, L. D. Unsworth, *Biointerphases* **2020**, *15*, 021007; c) X. J. Zhang, X. W. Wang, X. D. Da, Y. L. Shi, C. L. Liu, F. Sun, S. G. Yang, W. B. Zhang, *Biomacromolecules* **2018**, *19*, 1065.

[60] T. Christensen, W. Hassouneh, K. Trabbic-Carlson, A. Chilkoti, *Biomacromolecules* **2013**, *14*, 1514.

[61] M. Amiram, K. M. Luginbuhl, X. Li, M. N. Feinglos, A. Chilkoti, *Proc. Natl. Acad. Sci. USA* **2013**, *110*, 2792.

[62] M. K. McHale, L. A. Setton, A. Chilkoti, *Tissue Eng.* **2005**, *11*, 1768.

[63] T. Christensen, M. Amiram, S. Dagher, K. Trabbic-Carlson, M. F. Shamji, L. A. Setton, A. Chilkoti, *Protein Sci.* **2009**, *18*, 1377.

[64] K. Trabbic-Carlson, L. Liu, B. Kim, A. Chilkoti, *Protein Sci.* **2004**, *13*, 3274.

[65] T. Kowalczyk, K. Hnatuszko-Konka, A. Gerszberg, A. K. Kononowicz, *World J. Microbiol. Biotechnol.* **2014**, *30*, 2141.

[66] Y. H. Cho, Y. J. Zhang, T. Christensen, L. B. Sagle, A. Chilkoti, P. S. Cremer, *J. Phys. Chem. B* **2008**, *112*, 13765.

[67] D. E. Meyer, A. Chilkoti, *Nat. Biotechnol.* **1999**, *17*, 1112.

[68] W. Y. Wu, C. Mee, F. Califano, R. Banki, D. W. Wood, *Nat. Protoc.* **2006**, *1*, 2257.

[69] Y. Fan, J. M. Miozzi, S. D. Stimple, T.-C. Han, D. W. Wood, *Polymers* **2018**, *10*, 468.

[70] E. A. Golemis, E. Golemis, P. D. Adams, *Protein–Protein Interactions: A Molecular Cloning Manual*, Cold Spring Harbor Laboratory Press, New York **2002**.

[71] A. K. Varanko, J. C. Su, A. Chilkoti, *Annu. Rev. Biomed. Eng.* **2020**, *22*, 343.

[72] K. Trabbic-Carlson, D. E. Meyer, L. Liu, R. Piervincenzi, N. Nath, T. LaBean, A. Chilkoti, *Protein Eng., Des. Sel.* **2004**, *17*, 57.

[73] L. S. Nair, C. T. Laurencin, *Prog. Polym. Sci.* **2007**, *32*, 762.

[74] a) D. L. Nettles, A. Chilkoti, L. A. Setton, *Adv. Drug Delivery Rev.* **2010**, *62*, 1479; b) D. H. T. Le, A. Sugawara-Narutaki, *Mol. Syst. Des. Eng.* **2019**, *4*, 545.

[75] S. Gräslund, P. Nordlund, J. Weigelt, B. M. Hallberg, J. Bray, O. Gileadi, S. Knapp, U. Oppermann, C. Arrowsmith, R. Hui, J. Ming, S. dhe-Paganon, H.-w. Park, A. Savchenko, A. Yee, A. Edwards, R. Vincentelli, C. Cambillau, R. Kim, S.-H. Kim, Z. Rao, Y. Shi, T. C. Terwilliger, C.-Y. Kim, L.-W. Hung, G. S. Waldo, Y. Peleg, S. Albeck, T. Unger, O. Dym, et al., *Nat. Methods* **2008**, *5*, 135.

[76] Z. Chen, Q. Zhang, H. Li, Q. Wei, X. Zhao, F. Chen, *Bioact Mater* **2021**, *6*, 589.

[77] H. Betre, A. Chilkoti, L. A. Setton, presented at *Proc. of the Second Joint 24th Annual Conf. and the Annual Fall Meeting of the Biomedical Engineering Society*, Engineering in Medicine and Biology, XX October **2002**.

[78] D. L. Nettles, A. Chilkoti, L. A. Setton, *Adv. Drug Delivery Rev.* **2010**, *62*, 1479.

[79] M. Karimi, A. Ghasemi, P. S. Zangabad, R. Rahighi, S. M. M. Basri, H. Mirshekari, M. Amiri, Z. S. Pishabad, A. Aslani, M. Bozorgomid, D. Ghosh, A. Beyzavi, A. Vaseghi, A. R. Aref, L. Haghani, S. Bahrami, M. R. Hamblin, *Chem. Soc. Rev.* **2016**, *45*, 1457.

[80] a) S. Saha, S. Banskota, S. Roberts, N. Kirmani, A. Chilkoti, *Adv. Ther.* **2020**, *3*, 1900164; b) A. J. Simnick, C. A. Valencia, R. Liu, A. Chilkoti, *ACS Nano* **2010**, *4*, 2217.

[81] P. E. Wright, H. J. Dyson, *Nat. Rev. Mol. Cell Biol.* **2015**, *16*, 18.

[82] a) S. Roberts, M. Dzuricky, A. Chilkoti, *FEBS Lett.* **2015**, *589*, 2477; b) G. C. Yeo, F. W. Keeley, A. S. Weiss, *Adv. Colloid Interface Sci.* **2011**, *167*, 94; c) P. Tompa, M. Fuxreiter, *Trends Biochem. Sci.* **2008**, *33*, 2.

[83] a) M. Mann, O. N. Jensen, *Nat. Biotechnol.* **2003**, *21*, 255; b) C. T. Walsh, S. Garneau-Tsodikova, G. J. Gatto, *Angew. Chem., Int. Ed.* **2005**, *44*, 7342.

[84] A. Shah, M. S. Malik, G. S. Khan, E. Nosheen, F. J. Iftikhar, F. A. Khan, S. S. Shukla, M. S. Akhter, H. B. Kraatz, T. M. Aminabhavi, *Chem. Eng. J.* **2018**, *353*, 559.

[85] R. J. Mart, R. D. Osborne, M. M. Stevens, R. V. Ulijn, *Soft Matter* **2006**, *2*, 822.

[86] a) G. Z. Yang, D. Wibowo, J. H. Yun, L. Z. Wang, A. P. J. Middelberg, C. X. Zhao, *Langmuir* **2017**, *33*, 5777; b) D. Wibowo, H. F. Wang, Z. Z. Shao, A. P. J. Middelberg, C. X. Zhao, *J. Phys. Chem. C* **2017**, *121*, 14658; c) H. F. Wang, D. Wibowo, Z. Shao, A. P. J. Middelberg, C. X. Zhao, *Langmuir* **2017**, *33*, 7957; d) H. Z. Li, A. P. Le Brun, D. Agyei, W. Shen, A. P. J. Middelberg, L. Z. He, *J. Colloid Interface Sci.* **2016**, *462*, 56.

[87] a) D. Wibowo, G. Z. Yang, A. P. Middelberg, C. X. Zhao, *Biotechnol. Bioeng.* **2017**, *114*, 335; b) G. Yang, Y. Liu, Y. Hui, D. Chen, D. A. Weitz, C. X. Zhao, *Angew. Chem., Int. Ed.* **2021**, *60*, 15426; c) Tengjisi, Y. Liu, D. Zou, G. Yang, C.-X. Zhao, *J. Colloid Interface Sci.* **2022**, *624*, 242; d) Tengjisi, Y. Hui, G. Yang, G. Fu, Y. Liu, C.-X. Zhao, *J. Colloid Interface Sci.* **2021**, *581*, 185.

[88] Tengjisi, Y. Hui, Y. Fan, D. Zou, G. H. Talbo, G. Yang, C.-X. Zhao, *J. Colloid Interface Sci.* **2022**, *606*, 1737.

[89] D. Wibowo, C.-X. Zhao, A. P. J. Middelberg, *Chem. Commun.* **2014**, *50*, 11325.

[90] M. Dimitrijev Dwyer, M. Brech, L. Yu, A. P. J. Middelberg, *Chem. Eng. Sci.* **2014**, *105*, 12.

[91] Y. X. Sun, F. Ding, *Nanoscale* **2020**, *12*, 6307.

[92] G. A. Braun, B. E. Ary, A. J. Dear, M. C. H. Rohn, A. M. Payson, D. S. M. Lee, R. C. Parry, C. Friedman, T. P. J. Knowles, S. Linse, K. S. Åkerfeldt, *Biomacromolecules* **2020**, *21*, 4781.

[93] a) D. Ding, P. A. Guerette, S. Hoon, K. W. Kong, T. Cornvik, M. Nilsson, A. Kumar, J. Lescar, A. Miserez, *Biomacromolecules* **2014**, *15*, 3278; b) P. A. Guerette, S. Hoon, D. Ding, S. Amini, A. Masic, V. Ravi, B. Venkatesh, J. C. Weaver, A. Miserez, *ACS Nano* **2014**, *8*, 7170.

[94] P. A. Guerette, S. Hoon, Y. Seow, M. Raida, A. Masic, F. T. Wong, V. H. B. Ho, K. W. Kong, M. C. Demirel, A. Pena-Francesch, S. Amini, G. Z. Tay, D. Ding, A. Miserez, *Nat. Biotechnol.* **2013**, *31*, 908.

[95] a) S. H. Hiew, A. Miserez, *ACS Biomater. Sci. Eng.* **2017**, *3*, 680; b) A. Kumar, H. Mohanram, K. W. Kong, R. Goh, S. Hoon, J. Lescar, A. Miserez, *Biomater. Sci.* **2018**, *6*, 2440.

[96] a) T. J. Deming, in *Peptide Hybrid Polymers*, (Eds: H.-A. Klok, H. Schlaad), Springer, Berlin **2006**, p. 1; b) H. Schlaad, M. Antonietti, *Eur. Phys. J. E.* **2003**, *10*, 17.

[97] C. Dharmayanti, T. A. Gillam, M. Klingler-Hoffmann, H. Albrecht, A. Blencowe, *Polymers* **2021**, *13*, 624.

[98] a) P. Jing, J. S. Rudra, A. B. Herr, J. H. Collier, *Biomacromolecules* **2008**, *9*, 2438; b) R. I. Kühnle, D. Gebauer, H. G. Börner, *Soft Matter* **2011**, *7*, 9616; c) Z. Song, H. Fu, R. Wang, L. A. Pacheco, X. Wang, Y. Lin, J. Cheng, *Chem. Soc. Rev.* **2018**, *47*, 7401.

[99] C. Yang, Z. Shi, C. Feng, R. Li, S. Luo, X. Li, L. Ruan, *Macromol. Biosci.* **2020**, *20*, 2000034.

[100] a) P. Zhang, Z. Gao, J. Cui, J. Hao, *ACS Appl. Bio Mater.* **2020**, *3*, 561; b) Z. Guo, J. Sui, M. Ma, J. Hu, Y. Sun, L. Yang, Y. Fan, X. Zhang, *J. Controlled Release* **2020**, *326*, 350; c) J. Chen, J. Ding, Y. Zhang, C. Xiao, X. Zhuang, X. Chen, *Polym. Chem.* **2015**, *6*, 397; d) Z. Gao, Z. Zhang, J. Guo, J. Hao, P. Zhang, J. Cui, *Langmuir* **2020**, *36*, 13656; e) S. S. Han, Z. Y. Li, J. Y. Zhu, K. Han, Z. Y. Zeng, W. Hong, W. X. Li, H. Z. Jia, Y. Liu, R. X. Zhuo, X. Z. Zhang, *Small* **2015**, *11*, 2543.

[101] A. Q. Tao, G. Lo Huang, K. Igarashi, T. Hong, S. Y. Liao, F. Stellacci, Y. Matsumoto, T. Yamasoba, K. Kataoka, H. Cabral, *Macromol. Biosci.* **2020**, *20*, 1900161.

[102] a) N. Liu, B. Li, C. Gong, Y. Liu, Y. Wang, G. Wu, *Colloids Surf., B* **2015**, *136*, 562; b) B. Li, M. Shan, X. Di, C. Gong, L. Zhang, Y. Wang, G. Wu, *RSC Adv.* **2017**, *7*, 30242; c) J. J. Arroyo-Crespo, A. Armiñán, D. Charbonnier, L. Balzano-Nogueira, F. Huertas-López, C. Martí, S. Tarazona, J. Forteza, A. Conesa, M. J. Vicent, *Biomaterials* **2018**, *186*, 8.

[103] H. Takemoto, T. Inaba, T. Nomoto, M. Matsui, X. Liu, M. Toyoda, Y. Honda, K. Taniwaki, N. Yamada, J. Kim, K. Tomoda, N. Nishiyama, *Biomaterials* **2020**, *235*, 119804.

[104] C. Zhou, Z. Shi, F. Xu, Y. Ling, H. Tang, *Colloid Polym. Sci.* **2020**, *298*, 1293.

[105] S. J. Lee, K. H. Min, H. J. Lee, A. N. Koo, H. P. Rim, B. J. Jeon, S. Y. Jeong, J. S. Heo, S. C. Lee, *Biomacromolecules* **2011**, *12*, 1224.

[106] a. G D Rose, R. Wolfenden, *Annu. Rev. Biophys. Biomol. Struct.* **1993**, *22*, 381.

[107] S. S. Naik, J. G. Ray, D. A. Savin, *Langmuir* **2011**, *27*, 7231.

[108] a) C. Baldauf, R. Gunther, H. J. Hofmann, *Phys. Biol.* **2006**, *3*, S1; b) N. H. Shah, G. L. Butterfoss, K. Nguyen, B. Yoo, R. Bonneau, D. L. Rabenstein, K. Kirshenbaum, *J. Am. Chem. Soc.* **2008**, *130*, 16622; c) B. Paul, G. L. Butterfoss, M. G. Boswell, P. D. Renfrew, F. G. Yeung, N. H. Shah, C. Wolf, R. Bonneau, K. Kirshenbaum, *J. Am. Chem. Soc.* **2011**, *133*, 10910; d) Y.-U. Kwon, T. Kodadek, *J. Am. Chem. Soc.* **2007**, *129*, 1508; e) L. Guo, J. Li, Z. Brown, K. Ghale, D. Zhang, *Peptide Sci.* **2011**, *96*, 596; f) S. H. Lahasky, W. K. Serem, L. Guo, J. C. Garno, D. Zhang, *Macromolecules* **2011**, *44*, 9063.

[109] a) J. Sun, R. N. Zuckermann, *ACS Nano* **2013**, *7*, 4715; b) R. Luxenhofer, C. Fetsch, A. Grossmann, *J. Polym. Sci., Part A: Polym. Chem.* **2013**, *51*, 2731.

[110] S. Dai, P. Ravi, K. C. Tam, *Soft Matter* **2008**, *4*, 435.

[111] a) H. Tran, S. L. Gael, M. D. Connolly, R. N. Zuckermann, *J. Vis. Exp.* **2011**, *57*, e3373; b) W. Hua, Y. Wang, C.-Y. Guo, J. Wang, S. Li, L. Guo, *J. Inorg. Organomet. Polym. Mater.* **2021**, *31*, 203.

[112] a) L. Guo, D. Zhang, *J. Am. Chem. Soc.* **2009**, *131*, 18072; b) L. Guo, S. H. Lahasky, K. Ghale, D. Zhang, *J. Am. Chem. Soc.* **2012**, *134*, 9163.

[113] X. Tao, J. Du, Y. Wang, J. Ling, *Polym. Chem.* **2015**, *6*, 3164.

[114] S. Wang, Y. Tao, J. Wang, Y. Tao, X. Wang, *Chem. Sci.* **2019**, *10*, 1531.

[115] a) A. S. Culf, R. J. Ouellette, *Molecules* **2010**, *15*, 5282; b) R. N. Zuckermann, *Pept. Sci.* **2011**, *96*, 545.

[116] S. B. Y. Shin, K. Kirshenbaum, *Org. Lett.* **2007**, *9*, 5003.

[117] A. A. Fuller, F. J. Seidl, P. A. Bruno, M. A. Plescia, K. S. Palla, *Pept. Sci.* **2011**, *96*, 627.

[118] a) A. L. Calkins, J. Yin, J. L. Rangel, M. R. Landry, A. A. Fuller, G. Y. Stokes, *Langmuir* **2016**, *32*, 11690; b) A. A. Fuller, B. A. Yurash, E. N. Schaumann, F. J. Seidl, *Org. Lett.* **2013**, *15*, 5118.

[119] a) X. Bao, X. Si, X. Ding, L. Duan, C. Xiao, *J. Polym. Res.* **2019**, *26*, 278; b) Y.-B. Hu, E. B. Dammer, R.-J. Ren, G. Wang, *Transl. Neurodegener.* **2015**, *4*, 18; c) M. Stubbs, P. M. J. McSheehy, J. R. Griffiths, C. L. Bashford, *Mol. Med. Today* **2000**, *6*, 15.

[120] Y. Zhao, W. Ren, T. Zhong, S. Zhang, D. Huang, Y. Guo, X. Yao, C. Wang, W.-Q. Zhang, X. Zhang, Q. Zhang, *J. Controlled Release* **2016**, *222*, 56.

[121] T. Jiang, Z. Zhang, Y. Zhang, H. Lv, J. Zhou, C. Li, L. Hou, Q. Zhang, *Biomaterials* **2012**, *33*, 9246.

[122] a) C. Yu, L. Li, P. Hu, Y. Yang, W. Wei, X. Deng, L. Wang, F. R. Tay, J. Ma, *Adv. Sci.* **2021**, *8*, 2100540; b) X. Guo, X. Ling, F. Du, Q. Wang, W. Huang, Z. Wang, X. Ding, M. Bai, Z. Wu, *Transl Oncol* **2018**, *11*, 1065; c) M. A. Urello, L. Xiang, R. Colombo, A. Ma, A. Joseph, J. Boyd, N. Peterson, C. Gao, H. Wu, R. J. Christie, *Biomacromolecules* **2020**, *21*, 3596.

[123] A. Altunbas, S. J. Lee, S. A. Rajasekaran, J. P. Schneider, D. J. Pochan, *Biomaterials* **2011**, *32*, 5906.

[124] a) J. Sun, Q. Zheng, Y. Wu, Y. Liu, X. Guo, W. Wu, *J. Huazhong Univ. Sci. Technol., Med. Sci.* **2010**, *30*, 173; b) J. K. Tripathi, S. Pal, B. Awasthi, A. Kumar, A. Tandon, K. Mitra, N. Chattopadhyay, J. K. Ghosh, *Biomaterials* **2015**, *56*, 92; c) Z. Bian, J. Sun, *Int. J. Clin. Exp. Pathol.* **2015**, *8*, 1093; d) J. Sun, Q. Zheng, *J. Huazhong Univ. Sci. Technol., Med. Sci.* **2009**, *29*, 512.

[125] M. Gontsarik, A. Yaghmur, Q. Ren, K. Maniura-Weber, S. Salentinig, *ACS Appl. Mater. Interfaces* **2019**, *11*, 2821.

[126] Y. Kai-Larsen, B. Agerberth, *Front. Biosci.* **2008**, *13*, 3760.

[127] a) R. J. Mart, R. K. Allemann, *Chem. Commun.* **2016**, *52*, 12262; b) M. R. Jafari, H. T. Yu, J. M. Wickware, Y. S. Lin, R. Derda, *Org. Biomol. Chem.* **2018**, *16*, 7588.

[128] P. Zhang, M. Goswami, R. J. Zawadzki, E. N. PughJr., *Invest. Ophthalmol. Visual Sci.* **2016**, *57*, 3650.

[129] O. P. Narayan, X. Mu, O. Hasturk, D. L. Kaplan, *Acta Biomater.* **2021**, *121*, 214.

[130] a) T. Fehrentz, M. Schönberger, D. Trauner, *Angew. Chem., Int. Ed.* **2011**, *50*, 12156; b) W. A. Velema, W. Szymanski, B. L. Feringa, *J. Am. Chem. Soc.* **2014**, *136*, 2178.

[131] D. Bléger, S. Hecht, *Angew. Chem., Int. Ed.* **2015**, *54*, 11338.

[132] a) N. J. V. Lindgren, M. Varedian, A. Gogoll, *Chem. - Eur. J.* **2009**, *15*, 501; b) M. Varedian, M. Erdélyi, Å. Persson, A. Gogoll, *J. Pept. Sci.* **2009**, *15*, 107.

[133] a) T. Cordes, B. Heinz, N. Regner, C. Hoppmann, T. E. Schrader, W. Summerer, K. Rück-Braun, W. Zinth, *ChemPhysChem* **2007**, *8*, 1713; b) S. Wiedbrauk, H. Dube, *Tetrahedron Lett.* **2015**, *56*, 4266; c) T. Cordes, C. Elsner, T. T. Herzog, C. Hoppmann, T. Schadendorf, W. Summerer, K. Rück-Braun, W. Zinth, *Chem. Phys.* **2009**, *358*, 103.

[134] a) J. Zhao, D. Wildemann, M. Jakob, C. Vargas, C. Schiene-Fischer, *Chem. Commun.* **2003**, *22*, 2810; b) J. Helbing, H. Bregy, J. Bredenbeck, R. Pfister, P. Hamm, R. Huber, J. Wachtveitl, L. De Vico, M. Olivucci, *J. Am. Chem. Soc.* **2004**, *126*, 8823; c) Y. Huang, Z. Cong, L. Yang, S. Dong, *J. Pept. Sci.* **2008**, *14*, 1062; d) Z. Y. Cong, L. F. Yang, L. Jiang, D. Ye, S. L. Dong, *Chin. Chem. Lett.* **2010**, *21*, 476; e) J. M. Goldberg, S. Batjargal, E. J. Petersson, *J. Am. Chem. Soc.* **2010**, *132*, 14718.

[135] Y. Huang, G. Jahreis, C. Lücke, D. Wildemann, G. Fischer, *J. Am. Chem. Soc.* **2010**, *132*, 7578.

[136] a) K. Fujimoto, T. Maruyama, Y. Okada, T. Itou, M. Inouye, *Tetrahedron* **2013**, *69*, 6170; b) O. Babii, S. Afonin, M. Berditsch, S. Reißer, P. K. Mykhailiuk, V. S. Kubyshkin, T. Steinbrecher, A. S. Ulrich, I. V. Komarov, *Angew. Chem., Int. Ed.* **2014**, *53*, 3392.

[137] D. J. van Dijken, P. Kovaříček, S. P. Ihrig, S. Hecht, *J. Am. Chem. Soc.* **2015**, *137*, 14982.

[138] a) G. A. Woolley, *Acc. Chem. Res.* **2005**, *38*, 486; b) C. Renner, L. Moroder, *ChemBioChem* **2006**, *7*, 868.

[139] a) Z. Zhang, D. C. Burns, J. R. Kumita, O. S. Smart, G. A. Woolley, *Bioconjugate Chem.* **2003**, *14*, 824; b) D. C. Burns, F. Zhang, G. A. Woolley, *Nat. Protoc.* **2007**, *2*, 251.

[140] M. Dong, A. Babalhavaeji, S. Samanta, A. A. Beharry, G. A. Woolley, *Acc. Chem. Res.* **2015**, *48*, 2662.

[141] L. Guerrero, O. S. Smart, G. A. Woolley, R. K. Allemann, *J. Am. Chem. Soc.* **2005**, *127*, 15624.

[142] J. Yang, J.-I. Song, Q. Song, J. Y. Rho, E. D. H. Mansfield, S. C. L. Hall, M. Sambrook, F. Huang, S. Perrier, *Angew. Chem., Int. Ed.* **2020**, *59*, 8860.

[143] a) K. Deisseroth, *Nat. Methods* **2011**, *8*, 26; b) L. R. Polstein, C. A. Gersbach, *Nat. Chem. Biol.* **2015**, *11*, 198; c) T. A. Redchuk, M. M. Karasev, P. V. Verkhusha, S. K. Donnelly, M. Hülsemann, J. Virtanen, H. M. Moore, M. K. Vartiainen, L. Hodgson, V. V. Verkhusha, *Nat. Commun.* **2020**, *11*, 605; d) L. R. Polstein, C. A. Gersbach, *J. Am. Chem. Soc.* **2012**, *134*, 16480; e) D. Bracha, M. T. Walls, M. T. Wei, L. Zhu, M. Kurian, J. L. Avalos, J. E. Toettcher, C. P. Brangwynne, *Cell* **2018**, *175*, 1467.

[144] a) L. Albert, O. Vázquez, *Chem. Commun.* **2019**, *55*, 10192; b) K. Hüll, J. Morstein, D. Trauner, *Chem. Rev.* **2018**, *118*, 10710; c) S. Samanta, A. A. Beharry, O. Sadovski, T. M. McCormick, A. Babalhavaeji, V. Tropepe, G. A. Woolley, *J. Am. Chem. Soc.* **2013**, *135*, 9777.

[145] J. Chiefari, Y. Chong, F. Ercole, J. Krstina, J. Jeffery, T. P. Le, R. T. Mayadunne, G. F. Meijs, C. L. Moad, G. Moad, *Macromolecules* **1998**, *31*, 5559.

[146] P. J. Jervis, L. Hilliou, R. B. Pereira, D. M. Pereira, J. A. Martins, P. M. T. Ferreira, *Nanomaterials* **2021**, *11*, 704.

[147] N. P. Gabrielson, H. Lu, L. Yin, D. Li, F. Wang, J. Cheng, *Angew. Chem., Int. Ed.* **2012**, *51*, 1143.

[148] D. P. Morales, W. R. Wonderly, X. Huang, M. McAdams, A. B. Chron, N. O. Reich, *Bioconjugate Chem.* **2017**, *28*, 1816.

[149] R. F. Zou, Q. Wang, J. C. Wu, J. X. Wu, C. Schmuck, H. Tian, *Chem. Soc. Rev.* **2015**, *44*, 5200.

[150] E. A. Permiakov, *Metalloproteomics*, John Wiley & Sons, Hoboken, NJ **2009**.

[151] a) S. Zhang, *Nat. Biotechnol.* **2003**, *21*, 1171; b) D. E. Przybyla, J. Chmielewski, *Biochemistry* **2010**, *49*, 4411; c) M. Panciera, M. Amorín, J. R. Granja, *Chem. - Eur. J.* **2014**, *20*, 10260.

[152] J. C. Lewis, *ACS Catal.* **2013**, *3*, 2954.

[153] M. Albrecht, P. Stortz, *Chem. Soc. Rev.* **2005**, *34*, 496.

[154] B. Alies, C. Hureau, P. Faller, *Metallomics* **2013**, *5*, 183.

[155] a) D. M. Morgan, J. Dong, J. Jacob, K. Lu, R. P. Apkarian, P. Thiyagarajan, D. G. Lynn, *J. Am. Chem. Soc.* **2002**, *124*, 12644; b) J. Dong, J. E. Shokes, R. A. Scott, D. G. Lynn, *J. Am. Chem. Soc.* **2006**, *128*, 3540; c) H. Yang, M. Pritzker, S. Y. Fung, Y. Sheng, W. Wang, P. Chen, *Langmuir* **2006**, *22*, 8553; d) A. Jancsó, D. Szunyogh, F. H. Larsen, P. W. Thulstrup, N. J. Christensen, B. Gyurcsik, L. Hemmingsen, *Metallomics* **2011**, *3*, 1331; e) W. Hsu, Y. L. Chen, J. C. Horng, *Langmuir* **2012**, *28*, 3194; f) S. N. Dublin, V. P. Conticello, *J. Am. Chem. Soc.* **2008**, *130*, 49; g) K. Suzuki, H. Hiroaki, D. Kohda, H. Nakamura, T. Tanaka, *J. Am. Chem. Soc.* **1998**, *120*, 13008; h) A. Bavelloni, M. Piazzi, M. Raffini, I. Faenza, W. L. Blalock, *IUBMB Life* **2015**, *67*, 239.

[156] a) P. J. Knerr, M. C. Branco, R. Nagarkar, D. J. Pochan, J. P. Schneider, *J. Mater. Chem.* **2012**, *22*, 1352; b) G. R. Dieckmann, D. K. McRorie, J. D. Lear, K. A. Sharp, W. F. DeGrado, V. L. Pecoraro, *J. Mol. Biol.* **1998**, *280*, 897.

[157] a) Q. Dai, M. Prorok, F. J. Castellino, *J. Mol. Biol.* **2004**, *336*, 731; b) Q. Dai, C. Xiao, M. Dong, Z. Liu, Z. Sheng, F. J. Castellino, M. Prorok, *Peptides* **2009**, *30*, 866; c) Q. Dai, M. Dong, Z. Liu, M. Prorok, F. J. Castellino, *J. Inorg. Biochem.* **2011**, *105*, 52; d) W. D. Kohn, C. M. Kay, B. D. Sykes, R. S. Hodges, *J. Am. Chem. Soc.* **1998**, *120*, 1124.

[158] C. Tomasini, N. Castellucci, *Chem. Soc. Rev.* **2013**, *42*, 156.

[159] a) A. Krebs, V. Ludwig, J. Pfizer, G. Dürner, M. W. Göbel, *Chem. - Eur. J.* **2004**, *10*, 544; b) S. J. Zuend, M. P. Coughlin, M. P. Lalonde, E. N. Jacobsen, *Nature* **2009**, *461*, 968; c) R. J. Brea, M. P. López-Deber, L. Castedo, J. R. Granja, *J. Org. Chem.* **2006**, *71*, 7870.

[160] R. P. Cheng, S. L. Fisher, B. Imperiali, *J. Am. Chem. Soc.* **1996**, *118*, 11349.

[161] K. Dooley, B. Bulutoglu, S. Banta, *Biomacromolecules* **2014**, *15*, 3617.

[162] D. Ladant, A. Ullmann, *Trends Microbiol.* **1999**, *7*, 172.

[163] a) A. Chenal, J. C. Karst, A. C. S. Perez, A. K. Wozniak, B. Baron, P. England, D. Ladant, *Biophys. J.* **2010**, *99*, 3744; b) A.-C. Sotomayor-Pérez, D. Ladant, A. Chenal, *Toxins* **2015**, *7*, 1; c) M. A. Blenner, O. Shur, G. R. Szilvay, D. M. Cropek, S. Banta, *J. Mol. Biol.* **2010**, *400*, 244; d) G. R. Szilvay, M. A. Blenner, O. Shur, D. M. Cropek, S. Banta, *Biochemistry* **2009**, *48*, 11273.

[164] K. Dooley, Y. H. Kim, H. D. Lu, R. Tu, S. Banta, *Biomacromolecules* **2012**, *13*, 1758.

[165] a) H. Lilie, W. Haehnel, R. Rudolph, U. Baumann, *FEBS Lett.* **2000**, *470*, 173; b) T. Rose, P. Sebo, J. Bellalou, D. Ladant, *J. Biol. Chem.* **1995**, *270*, 26370; c) C. Bauche, A. Chenal, O. Knapp, C. Bodenreider, R. Benz, A. Chaffotte, D. Ladant, *J. Biol. Chem.* **2006**, *281*, 16914.

[166] L. Bumba, J. Masin, P. Macek, T. Wald, L. Motlova, I. Bibova, N. Klimova, L. Bednarova, V. Veverka, M. Kachala, *Mol. Cell* **2016**, *62*, 47.

[167] A. Chenal, J. I. Guijarro, B. Raynal, M. Delepierre, D. Ladant, *J. Biol. Chem.* **2009**, *284*, 1781.

[168] V. Kolenko, E. Teper, A. Kutikov, R. Uzzo, *Nat. Rev. Urol.* **2013**, *10*, 219.

[169] A. Takeda, H. Fujii, T. Minamino, H. Tamano, *J. Neurosci. Res.* **2014**, *92*, 819.

[170] a) A. Kyrychenko, M. M. Blazhynska, O. N. Kalugin, *J. Appl. Phys.* **2020**, *127*, 075502; b) D. H. Zhao, J. Yang, M. H. Yao, C. Q. Li, B. Zhang, D. Zhu, Y. D. Zhao, B. Liu, *Dalton Trans.* **2020**, *49*, 12049.

[171] X. Zhang, X. Zhang, M. Zhong, P. Zhao, C. Guo, Y. Li, H. Xu, T. Wang, H. Gao, *Int. J. Mol. Sci.* **2021**, *22*, 6842.

[172] J. Son, D. Kalafatovic, M. Kumar, B. Yoo, M. A. Cornejo, M. Contel, R. V. Ulijn, *ACS Nano* **2019**, *13*, 1555.

[173] A. S. Carlini, R. Gaetani, R. L. Braden, C. Luo, K. L. Christman, N. C. Gianneschi, *Nat. Commun.* **2019**, *10*, 14.

[174] D. S. MacPherson, S. A. McPhee, B. M. Zeglis, R. V. Ulijn, *ACS Biomater. Sci. Eng.* **2022**, *8*, 579.

[175] W. L. Zhang, C. E. Callmann, B. Meckes, C. A. Mirkin, *ACS Nano* **2022**, *16*, 10931.

[176] X. L. Jiang, X. B. Fan, W. Xu, C. G. Zhao, H. L. Wu, R. Zhang, G. Q. Wu, *J. Controlled Release* **2019**, *316*, 196.

[177] H. Wang, Y. Q. Hou, Y. L. Hu, J. X. Dou, Y. Q. Shen, Y. C. Wang, H. Lu, *Biomacromolecules* **2019**, *20*, 3000.

[178] S. J. Song, J. S. Choi, *Pharmaceutics* **2022**, *14*, 143.

[179] Y. J. Cheng, S. Y. Qin, W. L. Liu, Y. H. Ma, X. S. Chen, A. Q. Zhang, X. Z. Zhang, *Adv. Mater. Interfaces* **2020**, *7*, 9.

[180] Y. Ding, Z. Q. Sun, Z. R. Tong, S. T. Zhang, J. Min, Q. H. Xu, L. Z. Zhou, Z. W. Mao, H. B. Xia, W. L. Wang, *Theranostics* **2020**, *10*, 5195.

[181] X. K. Jin, H. Yang, Z. W. Mao, B. Wang, *J. Colloid Interface Sci.* **2021**, *601*, 714.

[182] H. N. He, L. Sun, J. X. Ye, E. G. Liu, S. H. Chen, Q. L. Liang, M. C. Shin, V. C. Yang, *J. Controlled Release* **2016**, *240*, 67.

[183] a) H. B. Yang, Z. Y. Yu, S. S. Ji, J. Yan, L. Han, Y. Liu, Y. J. Wang, Y. M. Niu, Q. Huo, M. Xu, *RSC Adv.* **2022**, *12*, 14707; b) L. Xu, X. Wang, Y. Liu, G. Yang, R. J. Falconer, C.-X. Zhao, *Adv. Nanobiomed. Res.* **2022**, *2*, 2100109; c) G. Yang, Y. Liu, S. Jin, C. X. Zhao, *ChemBioChem* **2020**, *21*, 2871.

[184] C. Battistella, C. E. Callmann, M. P. Thompson, S. Y. Yao, A. V. Yeldandi, T. Hayashi, D. A. Carson, N. C. Gianneschi, *Adv. Healthcare Mater.* **2019**, *8*, 5.

[185] S.-i. Yamamoto, J. Pietrasik, K. Matyjaszewski, *Macromolecules* **2008**, *41*, 7013.

[186] a) T. Shimoboji, E. Larenas, T. Fowler, S. Kulkarni, A. S. Hoffman, P. S. Stayton, *Proc. Natl. Acad. Sci. USA* **2002**, *99*, 16592; b) H.-i. Lee, J. Pietrasik, K. Matyjaszewski, *Macromolecules* **2006**, *39*, 3914.

[187] Y. Wang, L. Zhu, H. Zhang, H. Huang, L. Jiang, *Carbohydr. Polym.* **2020**, *241*, 116373.

[188] W. X. Lin, Y. J. Cui, Y. Yang, Q. Hu, G. D. Qian, *Dalton Trans.* **2018**, *47*, 15882.

[189] Y. Stetsyshyn, K. Fornal, J. Raczkowska, J. Zemla, A. Kostruba, H. Ohar, M. Ohar, V. Donchak, K. Harhay, K. Awsiuk, J. Rysz, A. Bernasik, A. Budkowski, *J. Colloid Interface Sci.* **2013**, *411*, 247.

[190] A. S. Culf, *Biopolymers* **2019**, *110*, 23285.

Yang Li received her bachelor's degree in Chemical and Biological Engineering (Class IA honors) from the University of Queensland in 2020. She is currently pursuing her Ph.D. degree in researching stimuli-responsive biomolecule-based surfactants funded by the Australian Research Council, Center of Excellence for Enabling Eco-Efficient Beneficiation of Minerals at the University of Queensland under the supervision of Prof. Chun-Xia Zhao. Her research focuses on designing stimuli-responsive peptides and proteins, mineral processing, chromatography, and expression and quantification of biomolecules.

Guangze Yang is currently a postdoctoral research fellow in the School of Chemical Engineering and Advanced Materials, The University of Adelaide (UofA). Before he joined UofA in 2022, he was a postdoctoral research fellow at the Australian Institute for Bioengineering and Nanotechnology (AIBN), the University of Queensland (UQ) from 2020 to 2022. He received his Ph.D. from AIBN, UQ in 2020. His research interests include peptide and protein design, nano-materials for drug delivery, and mineral processing.

Lukas Gerstweiler is a lecturer in bioprocess engineering at the University of Adelaide. His research focuses on advanced and intensified production technologies for industrial relevant proteins and biotherapeutics. In particular, he focuses on the transition from batch to continuous production, process integration, and advanced process control applying mechanistic and artificial intelligence based models.

San H. Thang is currently a Professor of Chemistry at Monash University, School of Chemistry. His research focuses on the interface between biology and polymer chemistry. He is responsible for several key inventions in the area of controlled/living radical polymerization; significantly, he is a coinventor of the RAFT (reversible addition–fragmentation chain transfer) process.

Chun-Xia Zhao is currently a professor and Australian National Health and Medical Research Council (NHMRC) Leadership Fellow at the School of Chemical Engineering and Advanced Materials, The University of Adelaide (UofA). She leads a research team focusing on the development of bioinspired micro/nanostructures for drug delivery and bioinspired devices (e.g., organs-on-a-chip models) for drug screening and evaluation. Prof. Zhao has published >110 publications in leading journals such as Science Advances, Nature Comm, Angewandte Chemie International Edition, ACS Nano, etc.